Charmonium-like exotic states at LHC

Results and prospects

A. Augusto Alves Jr, on behalf of the LHCb collaboration.
(Including results from CMS collaboration.)

University of Cincinnati
aalvesju@cern.ch

CHARM-2016, VIII International Workshop on Charm Physics
September 5 - 9, 2016, Bologna

Outline

1. The LHC accelerator and its detectors.
2. The LHCb detector.
3. Exotic states.
4. Results on pentaquark states on $\Lambda_b^0 \to J/\psi\, pK^-$ and $\Lambda_b^0 \to J/\psi\, p\pi^-$.
5. Search for structures in the $J/\psi\, \phi$ spectrum.

The LHC accelerator and its detectors

The LHC is designed to collide two high luminosity and high energy beams of protons or heavy ions.

- Two general proposal high luminosity experiments: CMS and ATLAS.
- One experiment dedicated to flavour physics: LHCb.
- Heavy-ion experiment: ALICE.

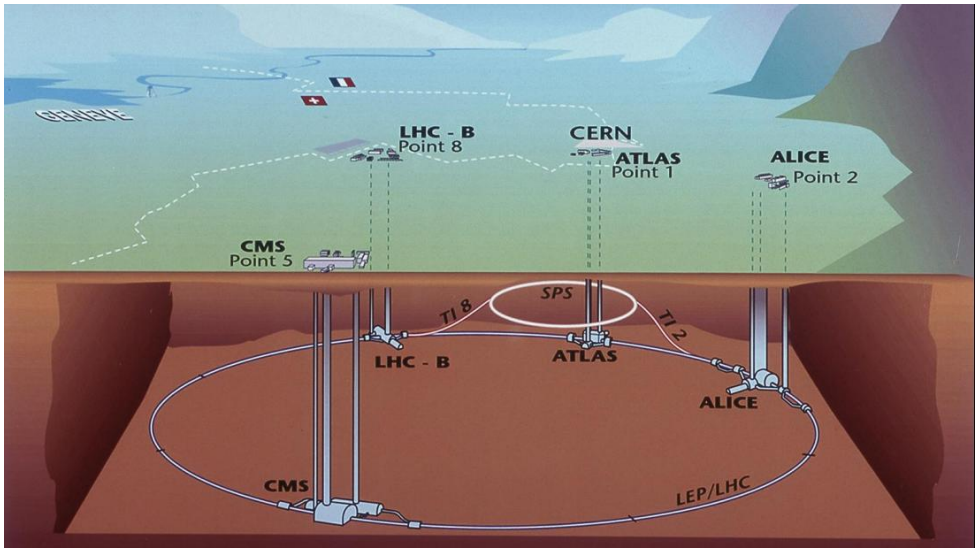

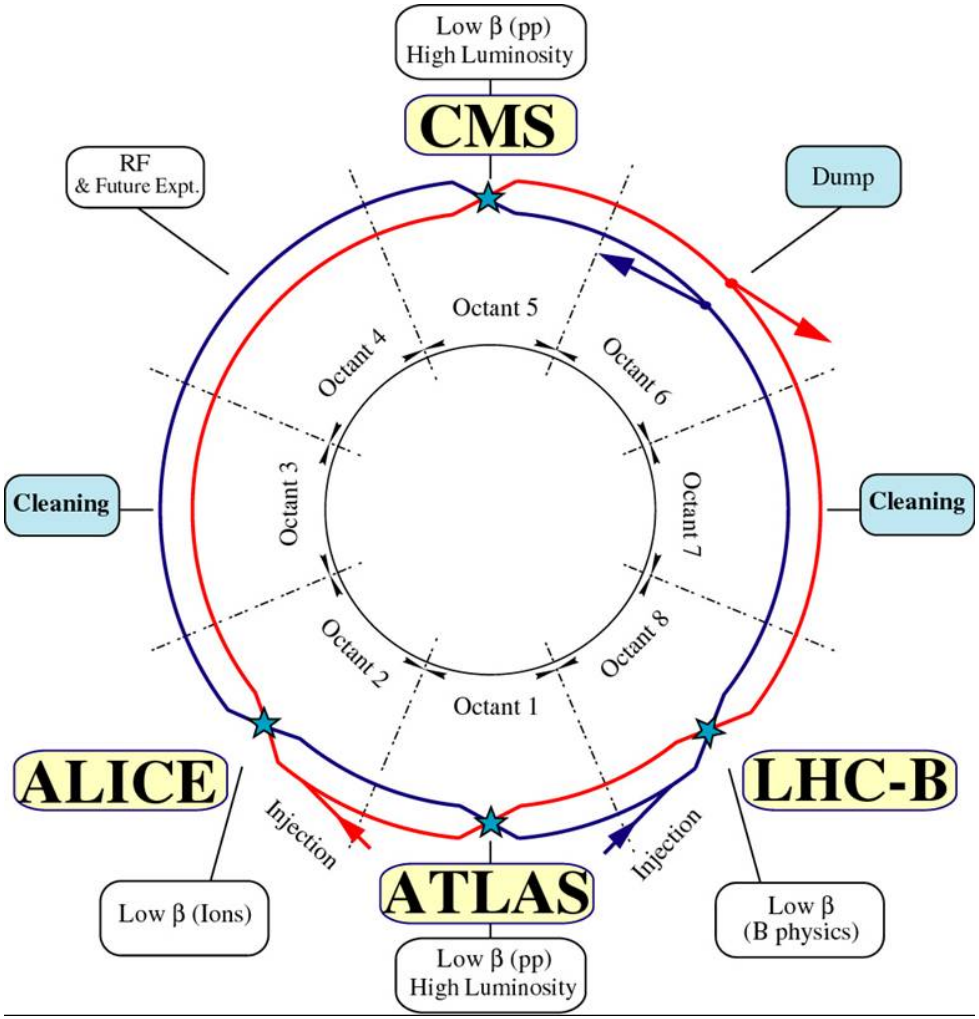

The LHC environment

During most of 2012 run, LHC collided protons at 8 TeV with an average instantaneous luminosity of $4 \times 10^{32} cm^{-2} s^{-1}$ (LHCb) and 20 MHz of bunch crossing.

- Inelastic cross section $\sim 60\,\mathrm{mb}$
- $\sigma(\mathrm{pp} \to \mathrm{b\bar{b}}X) = (284 \pm 20(\mathrm{stat}) \pm 49(\mathrm{syst}))\ \mu\mathrm{b}$ [PLB 694, 209]
- $\Longrightarrow$ $\sim 10^6$ $\mathrm{B\bar{B}}$ produced per second
- $\sigma(\mathrm{pp} \to c\bar{c}X)$ is about 20 times higher. [Nucl.Phys. B871 (2013) 1-20]

At the LHC energy, the $\mathrm{b\bar{b}}$ pairs are produced preferentially at forward (backward) directions.

- Optimal design is a forward detector: LHCb

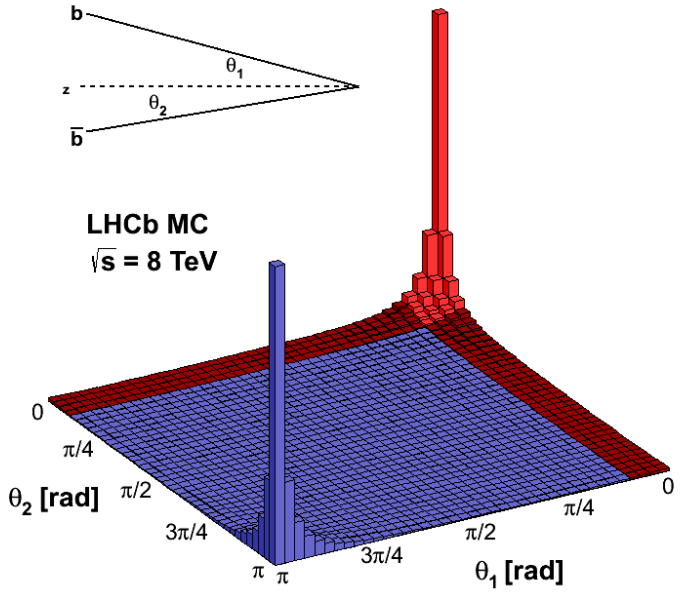

The LHCb detector

LHCb experiment was designed to perform high precision flavour physics measurements at the LHC.

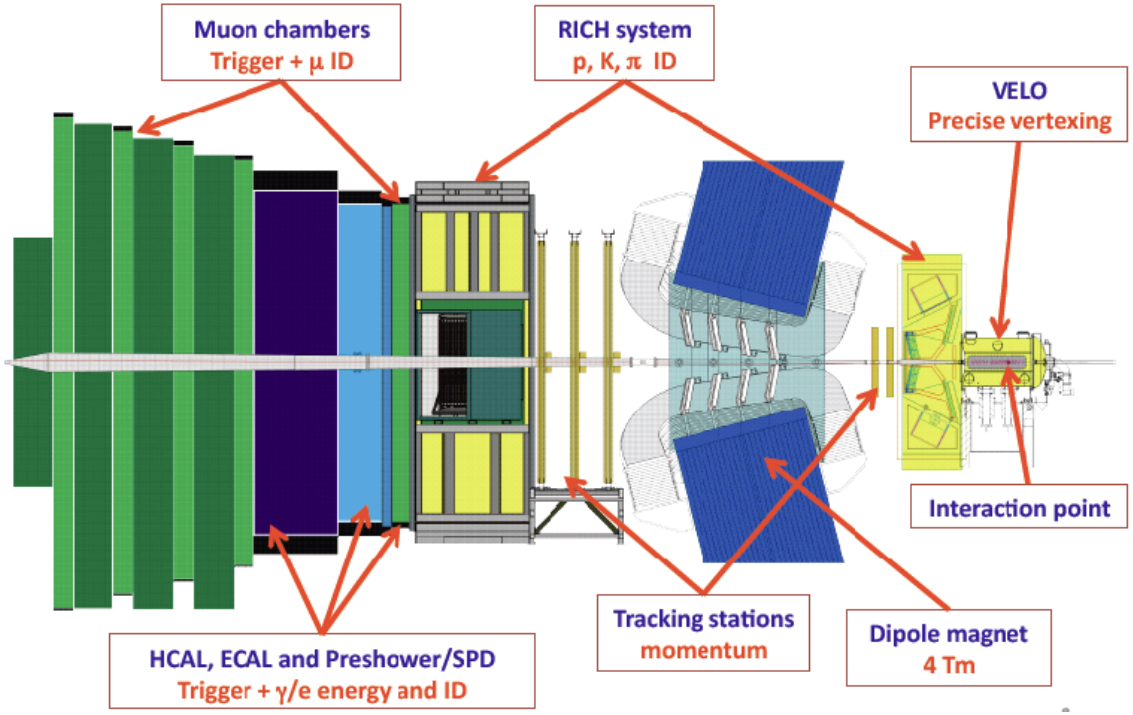

- **Single-arm design.** Covering the range $2 < \eta < 5$, LHCb can exploit the dominant heavy flavour production mechanism at the LHC and detects $\sim$ 40% of the $\mathrm{b\bar{b}}$ produced in forward region.
- **Good particle identification.** Excellent muon identification and good separation of π, K and p over (2 - 100) GeV.

- **Good vertexing and tracking.** Precise primary and secondary vertex reconstruction. Excellent momentum, IP and proper time resolution.
- These same features make LHCb very suitable for precision spectroscopy studies in the foward region.

The LHCb detector

Runs I and II

	Run I (2011 + 2012)	Run II (2016)
Bunch spacing	50ns	25ns
E_{cm}	7 TeV / 8 TeV	13 TeV
Luminosity	1 + 2 fb^{-1}	>5 fb^{-1}
Bunches	up to 1262	~2622

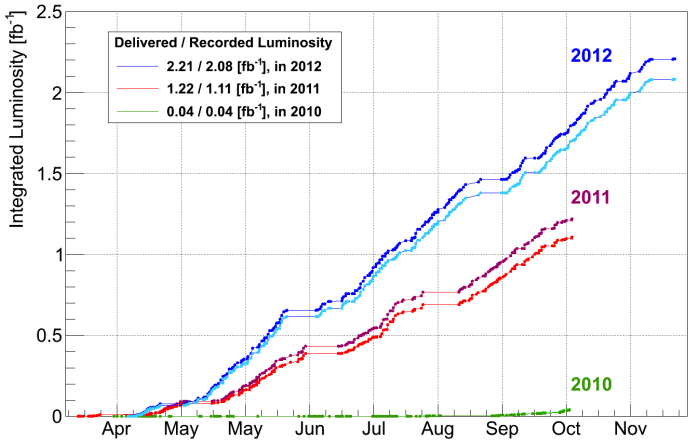

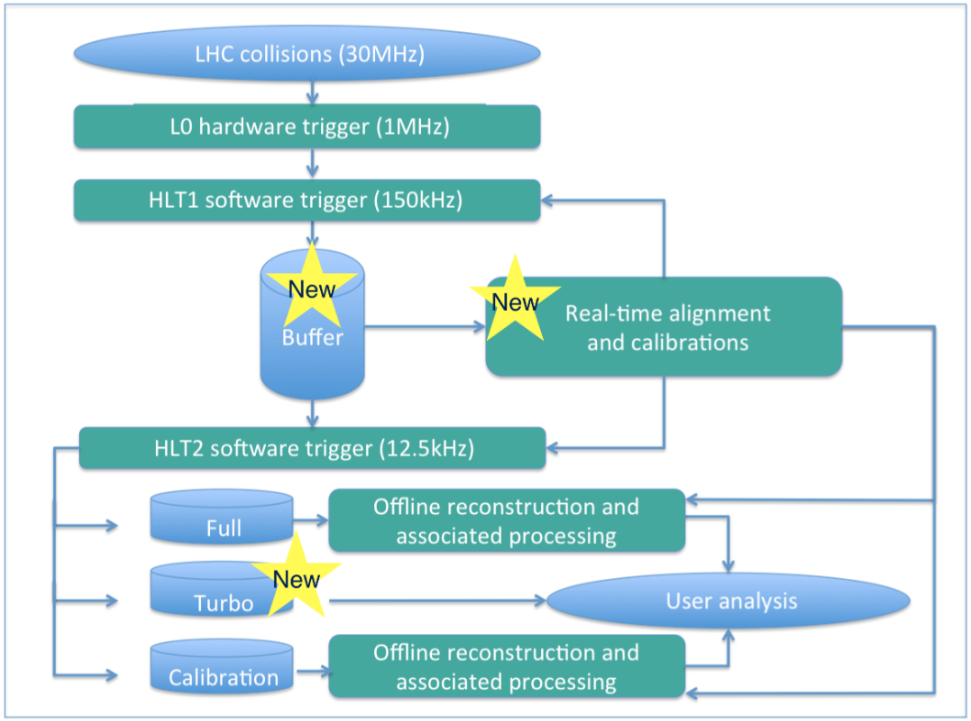

- The calibration and alignment process takes place now automatically online.
- The stored data are immediately available offline for physics analysis (turbo stream).
- The "turbo" data sample keeps only information necessary to perform physics analysis with the offline quality.
- Already 1 fb^{-1} recorded in RUNII/2015 and increasing.

XYZ states

Many new states have been observed at Charm, b-factories and Tevatron:

- Masses lying on the limits of the quarkonia spectrum.
- Observed many different production mechanisms: ISR, e^+e^-, $\gamma\gamma$ and B decays.
- The measured masses do not correspond to the predicted values for conventional quarkonia.
- The properties do not fit very well to the quarkonia picture.

Many theoretical interpretations in discussion:

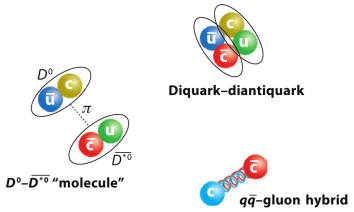

- conventional quarkonia;
- multiquark states;
- meson-molecules;
- hybrid mesons;
- threshold effects;

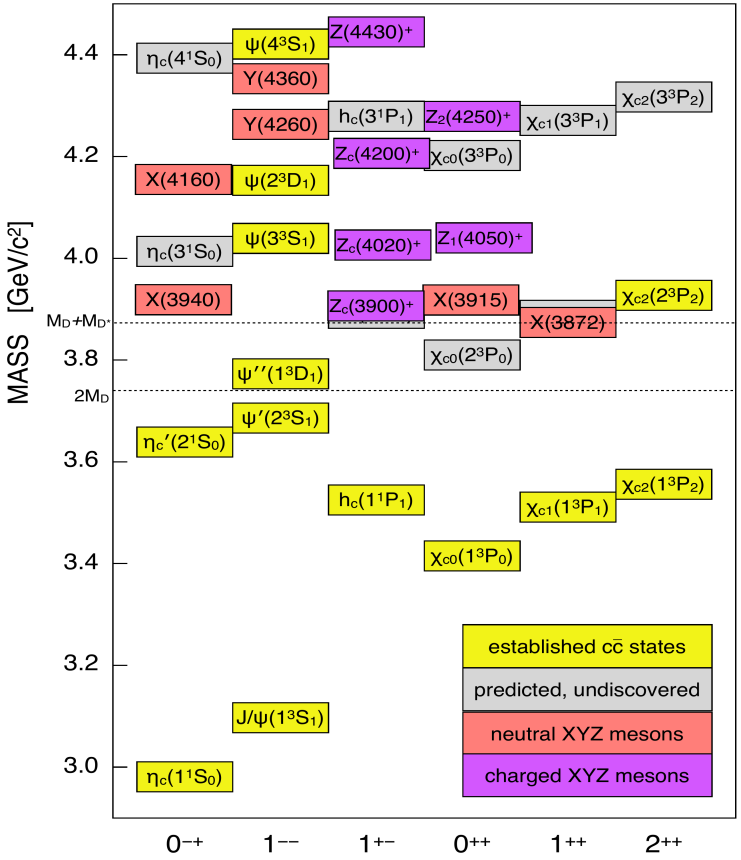

[PoS Bormio 050(2015) arXiv:1511.01589]

The table should be updated to include some new states: $P(4380)_c^+$, $P(4450)_c^+$ ...

Pentaquark states in $\Lambda_b^0 \to J/\psi\, pK^-$

Phys. Rev. Lett. 115 (2015) 072001

- Sample with >26.000 $\Lambda_b^0 \to J/\psi\, pK^-$ signal candidates,
- Analysis: six-dimensional amplitude fit (invariant masses, helicity and decay planes angles).
- Background from sidebands. Estimated 5.4% of combinatorial background in the signal region.
- Six-dimensional efficiency calculated using complete simulation of the detector.

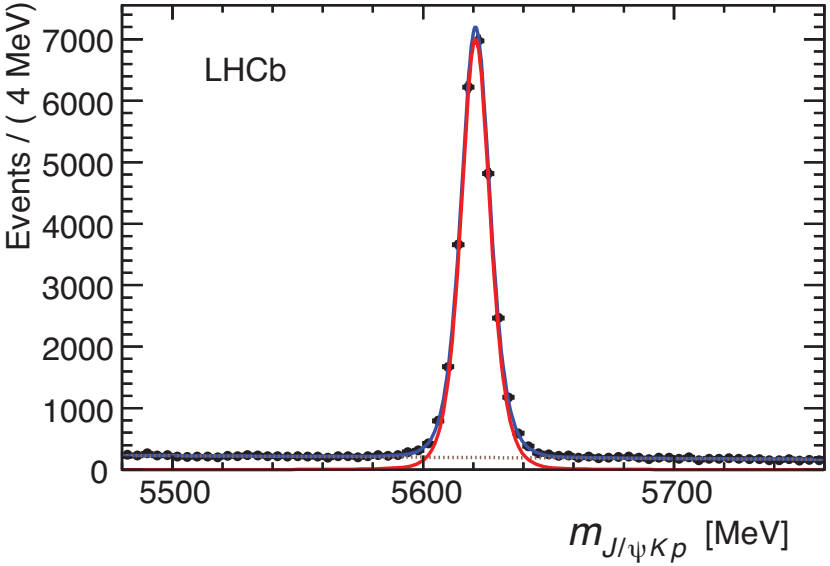

background subtracted Dalitz plot

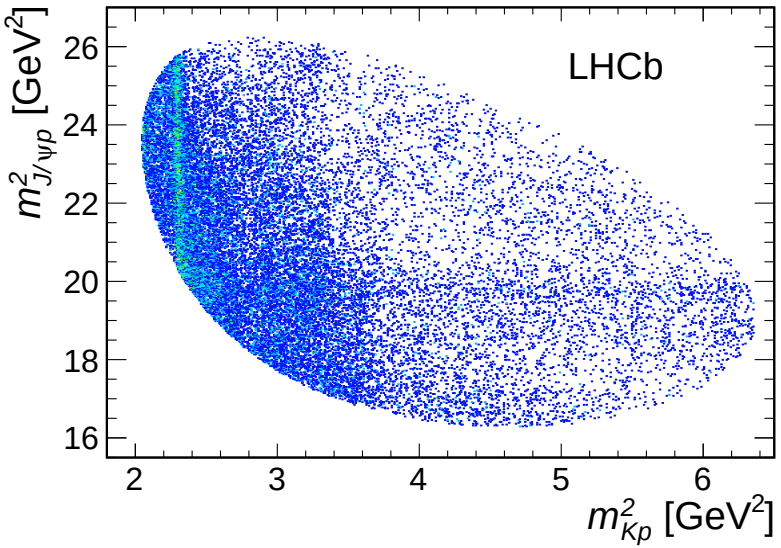

Pentaquark states in $\Lambda_b^0 \to J/\psi\, pK^-$

Some analysis details

- Two parametrizations: $\Lambda_b^0 \to K^-(P_c^+ \to pJ/\psi)$ and $\Lambda_b^0 \to J/\psi(\Lambda^* \to pK^-)$, with $J/\psi \to \mu^+\mu^-$

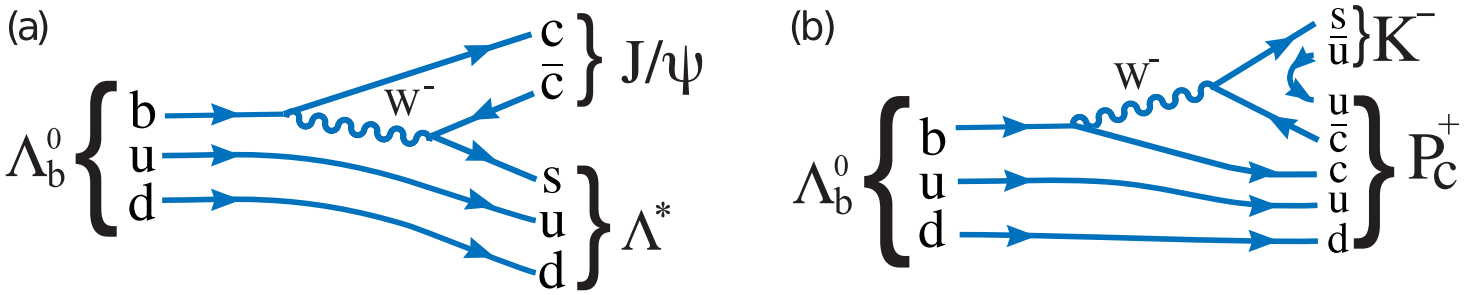

- Six-dimensional amplitude fit. Resonance invariant mass, three helicities angles, and two differences between decay planes.

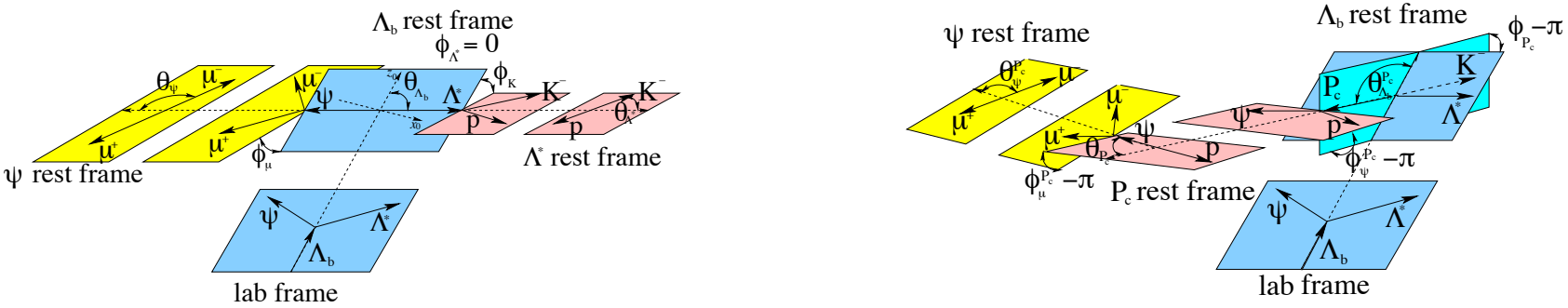

- Lorentz transformations relates the two helicity representantions.
- Resonances described by Breit-Wigner.
- Angular distribution calculated using helicity formalism.

Pentaquark states in $\Lambda_b^0 \to J/\psi\, pK^-$

Fit results with pentaquark states

- Fit including just well motivated Λ^* resonances (Reduced model).
- Two P_c^+ states necessary to achieve acceptable fit quality.
- $P(4380)_c^+$ with $M = 4380 \pm 8 \pm 29\,\mathrm{MeV}/c^2$ and $\Gamma = 205 \pm 18 \pm 86\,\mathrm{MeV}/c^2$ $J^P = 3/2^-$, fit fraction of $(8.4 \pm 0.7 \pm 4.2)\%$ and significance of 9σ
- $P(4450)_c^+$ with $M = 4449.8 \pm 1.7 \pm 2.5\,\mathrm{MeV}/c^2$ and $\Gamma = 39 \pm 5 \pm 19\,\mathrm{MeV}/c^2$ $J^P = 5/2^+$, fit fraction $(4.1 \pm 0.5 \pm 1.1)\%$ and significance of 12σ
- The mass resolution is approximately $2.5\,\mathrm{MeV}/c^2$ and combined significance 15σ

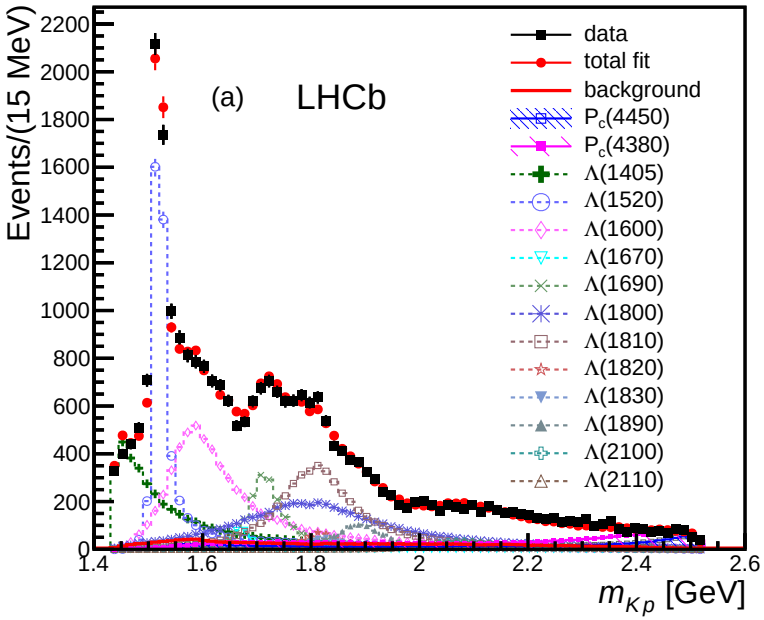

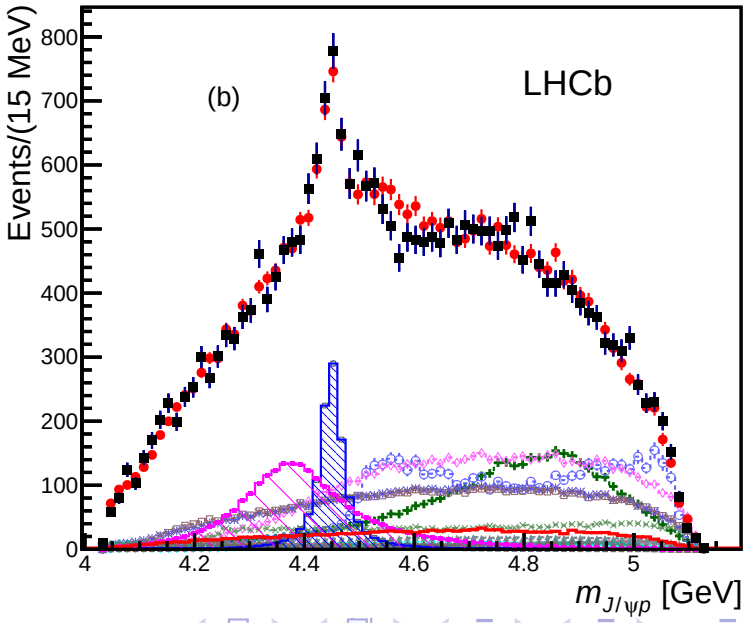

Pentaquark states in $\Lambda_b^0 \to J/\psi\, pK^-$

Resonant character of the pentaquark states

- $P(4450)_c^+$ amplitude is now described by 6 independent complex numbers instead of a Breit-Wigner.
- Six equidistant points in the range $\pm\Gamma_0 = 39\,\mathrm{MeV}/c^2$ around $M_0 = 4449.8\,\mathrm{MeV}/c^2$ (from the default fit).
- Observe a fast change of phase crossing maximum of magnitude. Expected behavior for a resonance.
- Same test on $P(4380)_c^+$ leads to inconclusive results.

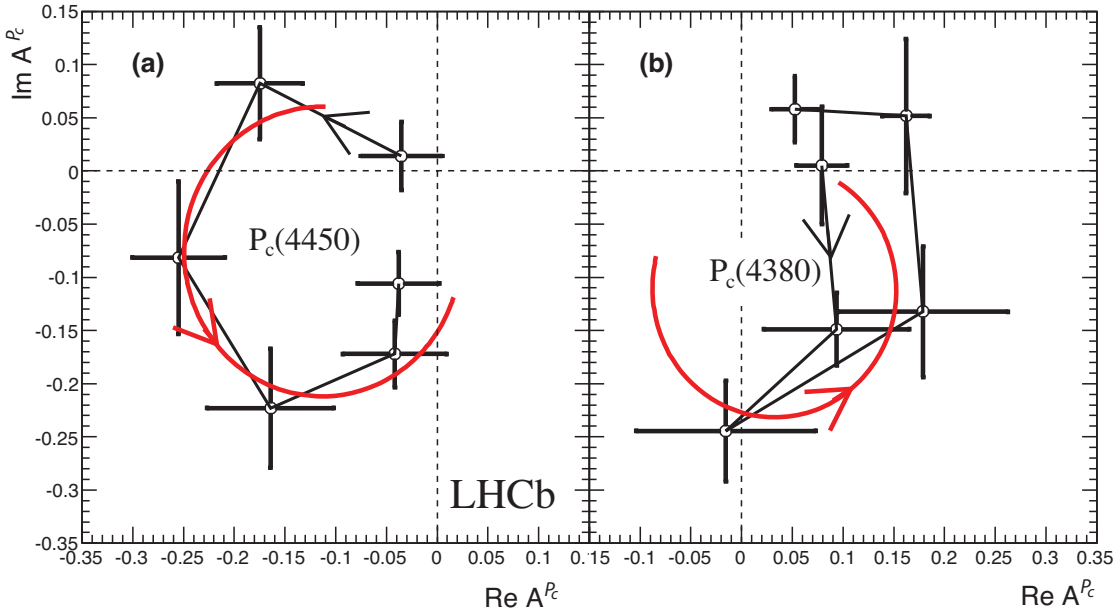

Pentaquark states in $\Lambda_b^0 \to J/\psi\, pK^-$

Model independent analysis [Phys. Rev. Lett. 117, 082002 (2016)]

- The goal of this analysis approach is explain the structures observed in the pJ/ψ invariant mass as a reflections of the activity of the conventional resonances on the K^-p system.
- No model dependent assumptions are made. Instead, the m_{K^-p} distribution is taken from data as it is.
- The angular structure of the K^-p system is acquired via Legendre polynomials calculated from the Λ^* helicity angle.
- This method was introduced by the BaBar collaboration and later improved upon by the LHCb collaboration, both in the context of the search for $Z(4430)^+$ on $B^0 \to \psi(2S)K^+\pi^-$ decays.

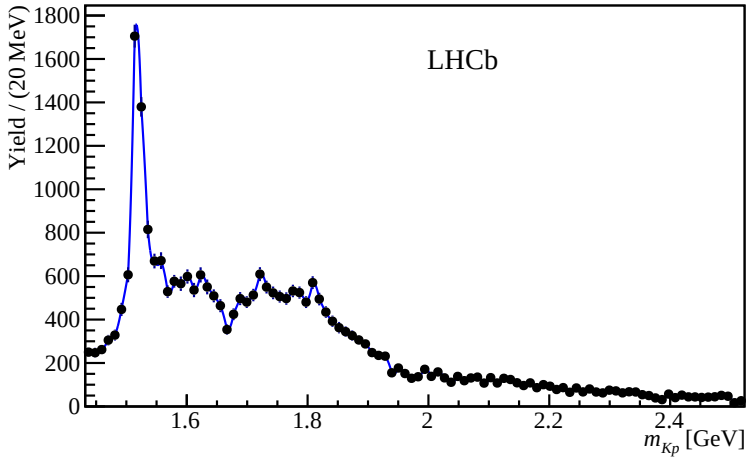

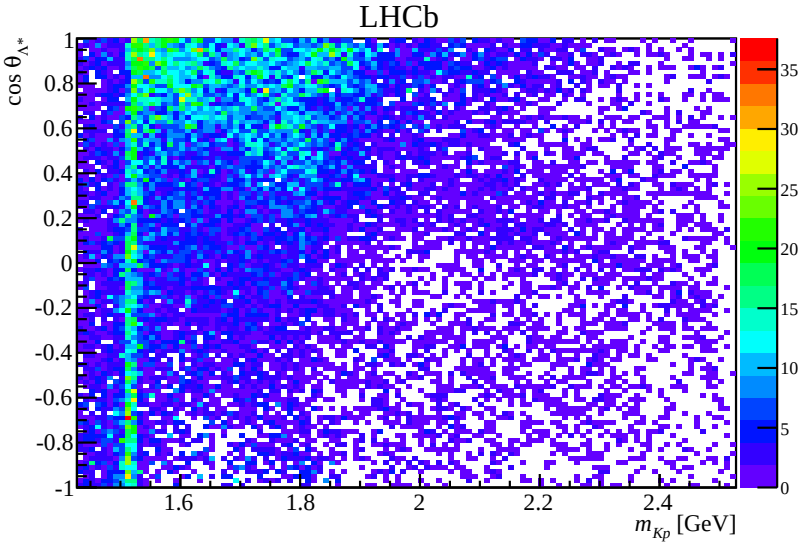

Pentaquark states in $\Lambda_b^0 \to J/\psi\, pK^-$

Model independent analysis: Legendre polynomials

- The maximum order of the Legendre polynomials considered in each m_{K^-p} slice is limited by the maximum spin of the Λ^* expected to give local contributions.
- A normalized weight is calculated and used to reweight simulated events to obtain a prediction for $m_{J/\psi\, p}$ distribution consistent with the conventional resonances contributions.
- The predicted distribution does not provide a satisfactory description of LHCb data.

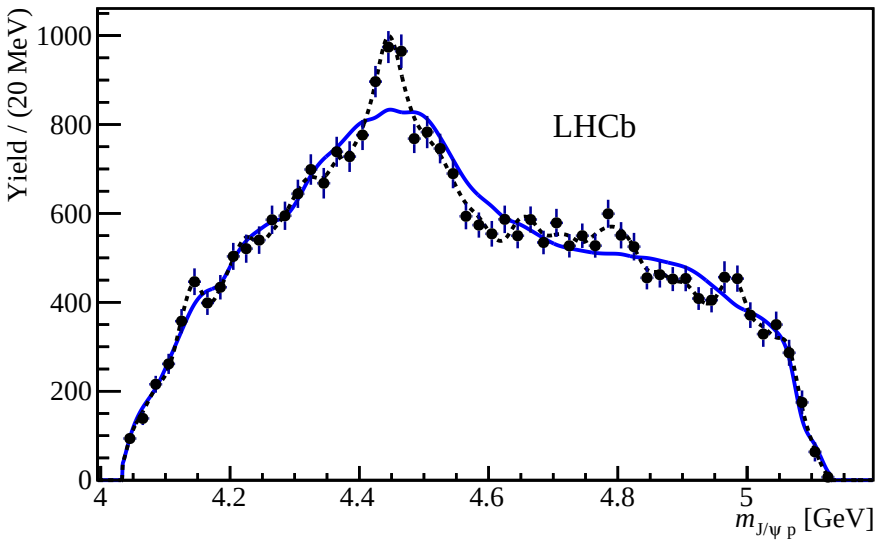

Legendre polynomials in function of m_{K^-p}. Yellow shadowed areas are filtered out.

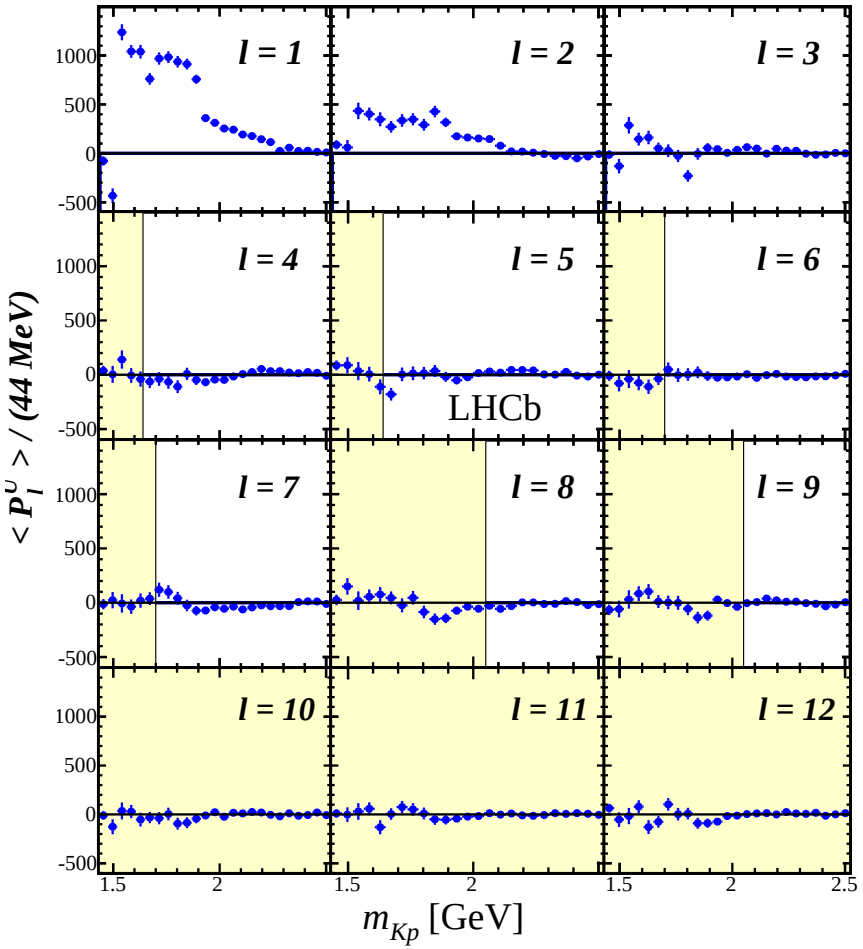

Evidence for exotic hadron contributions to $\Lambda_b^0 \to J/\psi\, p\pi^-$

Phys. Rev. Lett. 117 (2016) 082003

- Sample with 1885 ± 50 $\Lambda_b^0 \to J/\psi\, p\pi^-$ signal candidates,
- Analysis: six-dimensional amplitude fit (invariant masses, helicity and decay planes angles).
- Combinatorial background modeled by an exponential function and events from $\Lambda_b^0 \to J/\psi\, pK^-$ modeled using simulated samples.
- Six-dimensional efficiency calculated using complete simulation of the detector.

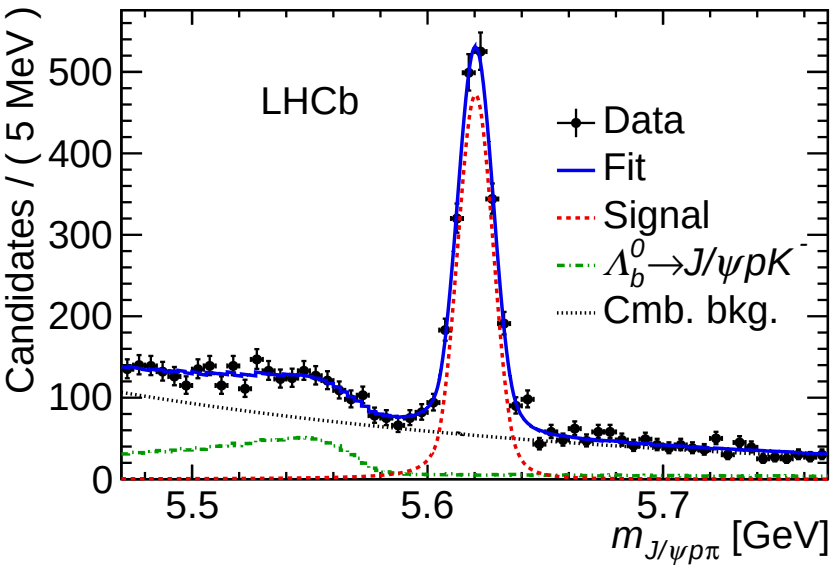

background subtracted Dalitz plot

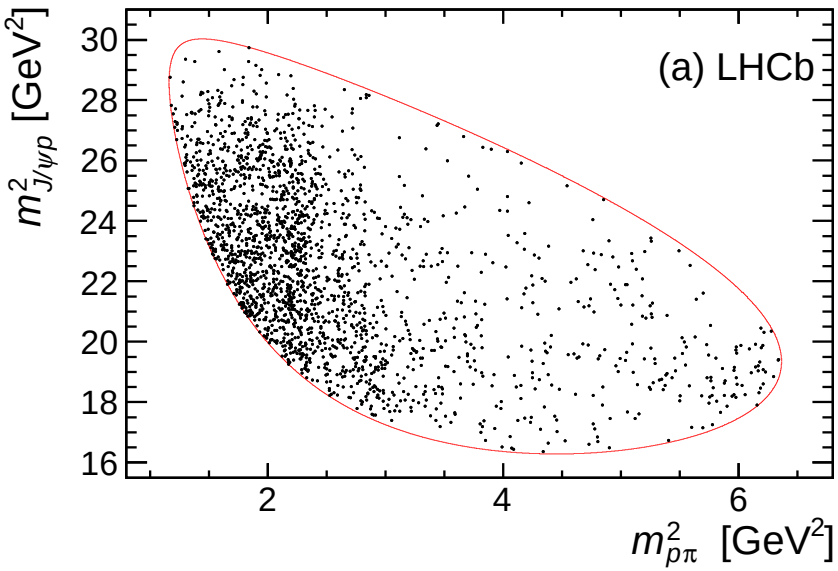

Evidence for exotic hadron contributions to $\Lambda_b^0 \to J/\psi\, p\pi^-$

Some analysis details

- Three parametizations: $\Lambda_b^0 \to (P_c^+ \to J/\psi\, p)\pi^-$, $\Lambda_b^0 \to (Z_c(4200)^+ \to J/\psi\, \pi^-)p$ and $\Lambda_b^0 \to J/\psi\,(N^* \to p\pi^-)$, with $J/\psi \to \mu^+\mu^-$.
- Six-dimensional amplitude fit: resonance invariant mass, three helicities angles, and two differences between decay planes.
- Lorentz transformations relates the two helicity representantions.

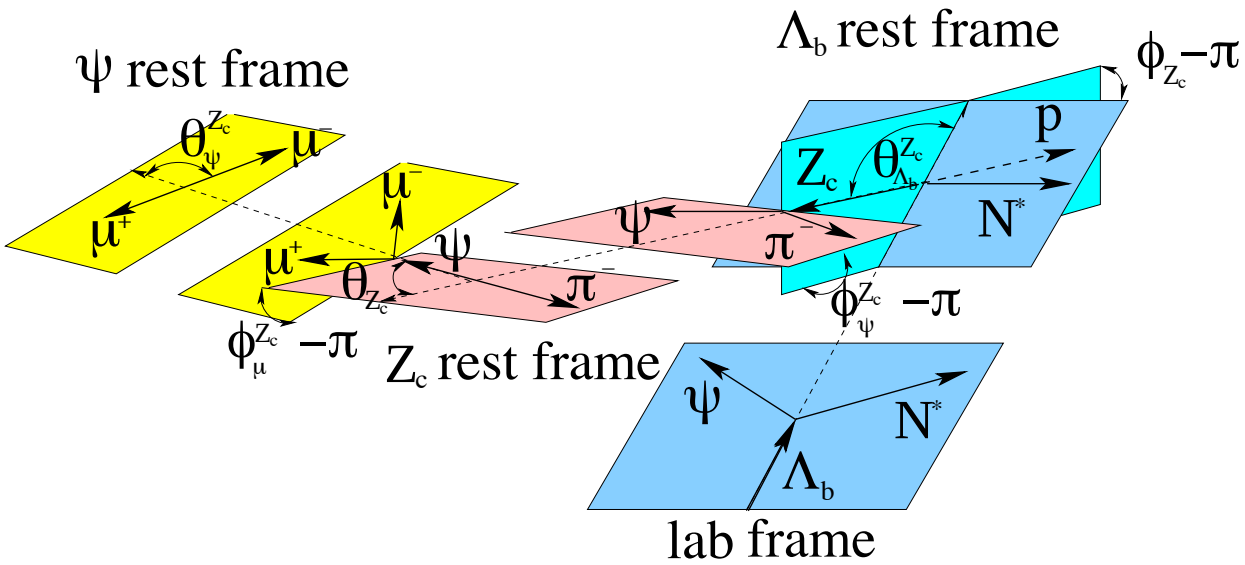

- Resonances described by Breit-Wigner.
- Angular distribution calculated using helicity formalism.

Evidence for exotic hadron contributions to $\Lambda_b^0 \to J/\psi\, p\pi^-$

Amplitude analysis

- Reduced Model. Including only well estabilished N^* resonances.
- Extended Model. Used to calculate systematic uncertainties and the significances.
- Exotic states contributions are necessary to achieve acceptable fit quality, mainly in the $m_{p\pi^-} > 1.8\,\mathrm{GeV}/c^2$ region.

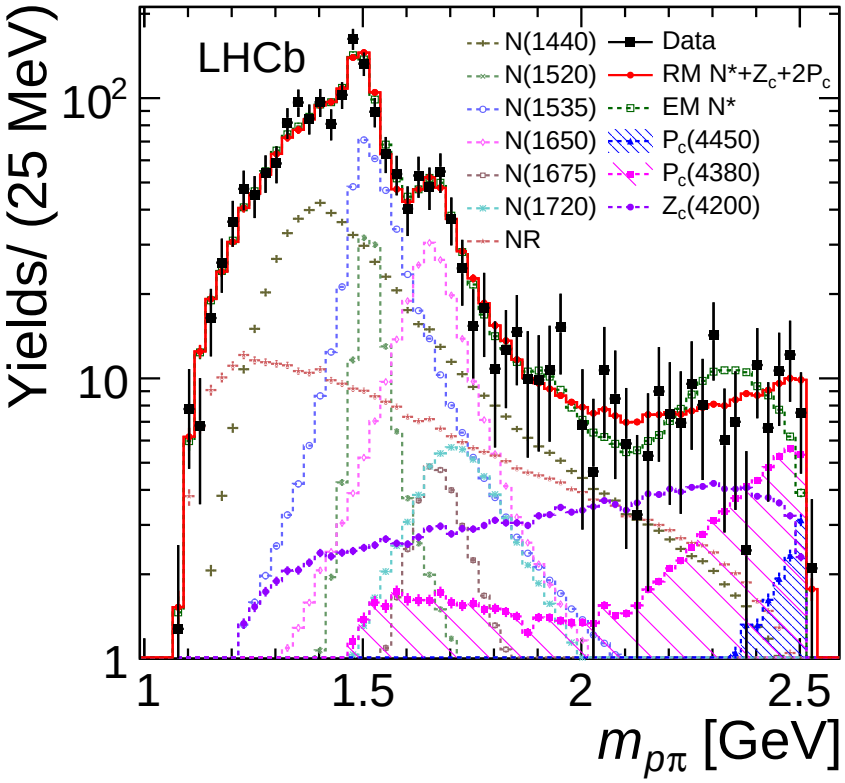

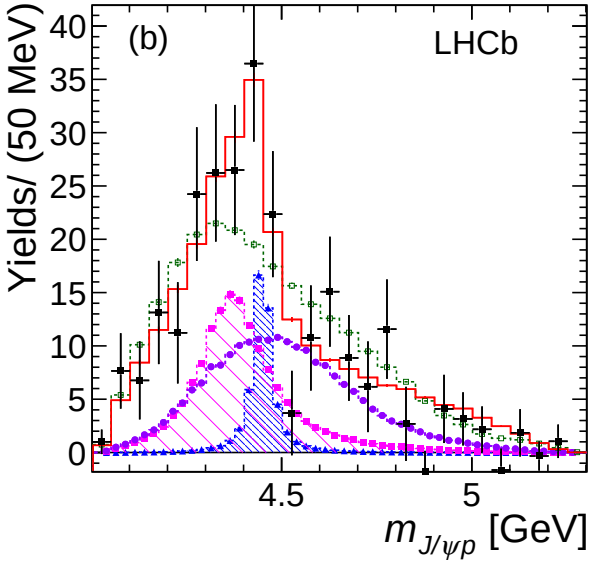

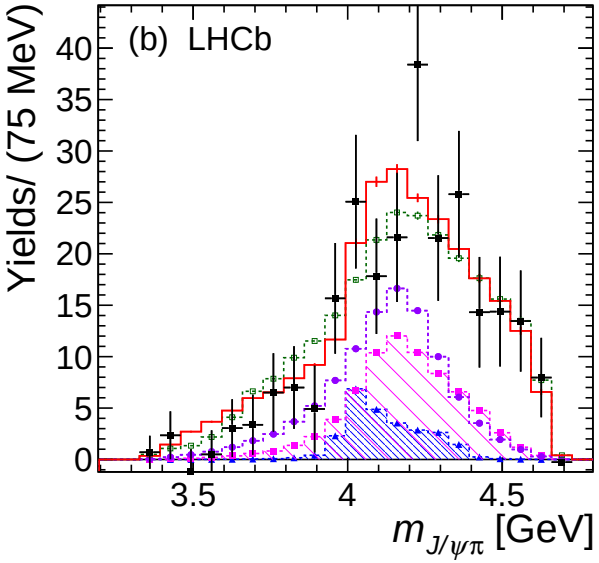

Evidence for exotic hadron contributions to $\Lambda_b^0 \to J/\psi\, p\pi^-$

Results

- Fit fractions from the RM + exotic states.
  - $P(4380)_c^+$: $(5.1 \pm 1.5^{+2.6}_{-1.6})\%$
  - $P(4450)_c^+$: $(1.6^{+0.8+0.6}_{-0.6-0.5})\%$
  - $Z_c(4200)^+$: $(7.7 \pm 2.8^{+3.4}_{-4.0})\%$
- When the two P_c^+ states are not considered, the fraction for the $Z_c(4200)^+$ state is $(17.2 \pm 3.5)\%$.
- Conversely, the fit fractions of the two P_c^+ states remain stable regardless of the inclusion of the $Z_c(4200)^+$ state.
- If both types of exotic resonances are included, the total significance for them is 3.1σ.
- Assuming that the $Z_c(4200)^+$ contribution is negligible, there is a 3.3σ significance for the two P_c^+ states taken together.

The $X(4140)$ and $X(4274)$

- Two exotic resonance candidates observed by CDF in $B^{\pm} \to J/\psi\,\phi K^{\pm}$ decays and decaying into $J/\psi\,\phi$. [Ref. Phys.Rev.Lett. 102.242002].
- D0 experiment also reported the observation of structures on $J/\psi\,\phi$ invariant mass on B decays and promp candidates. [Ref. Phys. Rev. D 89, 012004, arXiv:1508.07846].
- Belle experiment also have searched for $X(4140)$ and $X(4274)$. Belle accumulated more events on $B^{\pm} \to J/\psi\,\phi K^{\pm}$ than CDF but could not confirm or exclude the $X(4140)$. due loss of efficiency near the threshold, which resulted in a lower sensitivity to $X(4140)$. [see J. Brodzicka, Heavy flavour spectroscopy (LP09)]

In summary:

- Charmonium states at this mass are expected to have much larger widths because of open flavour decay channels.
- Their decay rate into the $J/\psi\,\phi$ mode (so near the kinematic threshold) should be small and unobservable.
- This make $X(4140)$ and $X(4274)$ strongly exotic chamornium-like candidates.

Search for structures in the $J/\psi\,\phi$ spectrum at CMS

Phys. Lett. B 734 (2014) 261

- Analysis performed on a sample of 2480 ± 160 $B^{\pm} \to J/\psi\,\phi K^{\pm}$ signal candidates.
- $J/\psi\,\phi$-spectrum is modeled by two S-wave relativistic Breit-Wigner over a three-body phase-space non-resonant component.
- $m_1 = 4148.2 \pm 2.4(\mathrm{stat}) \pm 6.3(\mathrm{syst})\,\mathrm{MeV}/c^2$, $\Gamma_1 = 28^{+15}_{-11}(\mathrm{stat}) \pm 19(\mathrm{syst})\,\mathrm{MeV}/c^2$, and significance exceeding $5\,\sigma$.
- $m_2 = 4313.8 \pm 5.3(\mathrm{stat}) \pm 7.3(\mathrm{syst})\,\mathrm{MeV}/c^2$ and $\Gamma_2 = 38^{+30}_{-15}(\mathrm{stat}) \pm 16(\mathrm{syst})\,\mathrm{MeV}/c^2$.

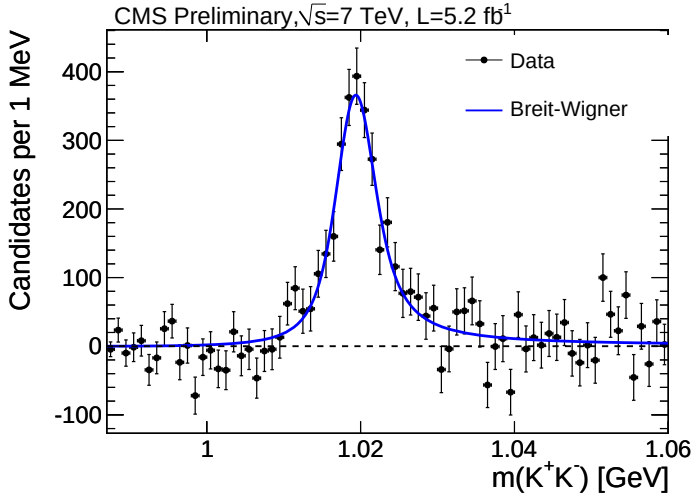

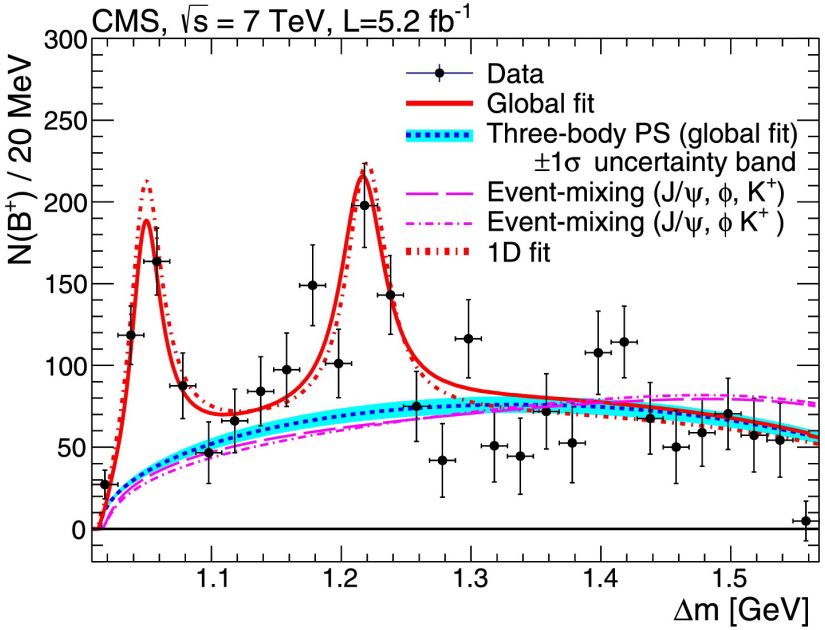

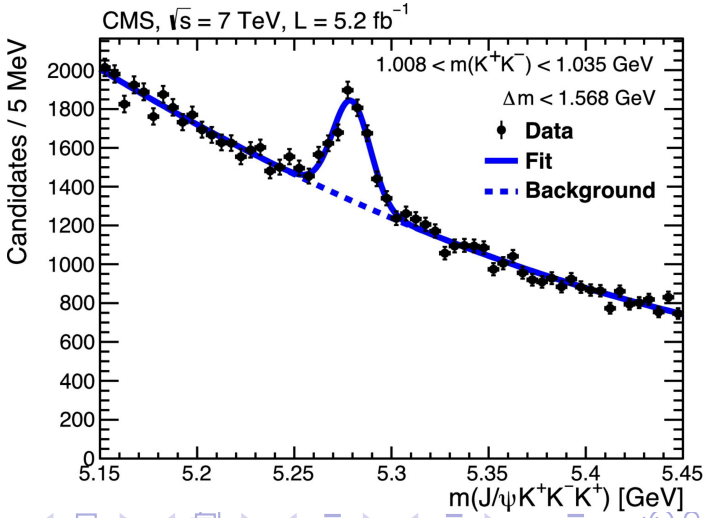

Search for structures in the $J/\psi\,\phi$ spectrum at LHCb

arXiv:1606.07898, arXiv:1606.07895

- Sample with 4289 ± 151 $B^{\pm} \to J/\psi\,\phi K^{\pm}$ with $J/\psi \to \mu^+\mu^-$ and and $\phi \to K^+K^-$ signal candidates.
- Analysis: six-dimensional amplitude fit (invariant masses, helicity and decay planes angles).
- Background from sidebands. Estimated $(23 \pm 6)\%$ of combinatorial background in the signal region.
- Six-dimensional efficiency calculated using complete simulation of the detector.

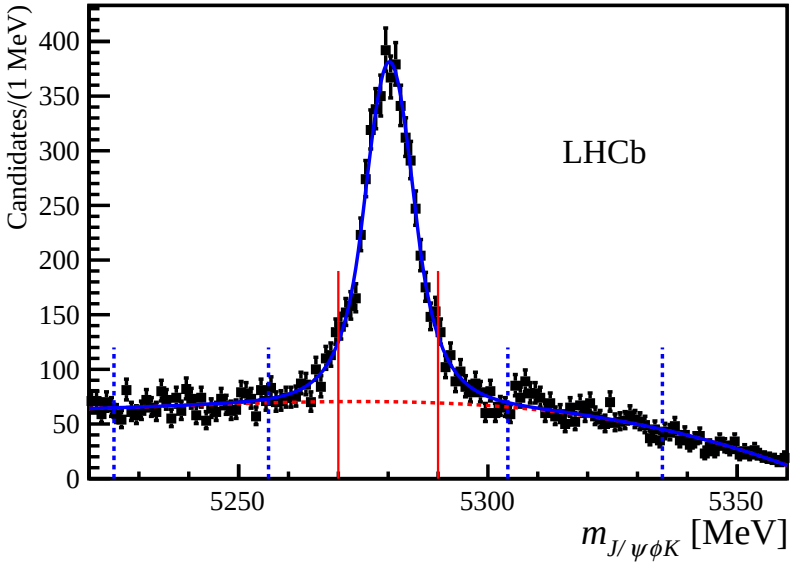

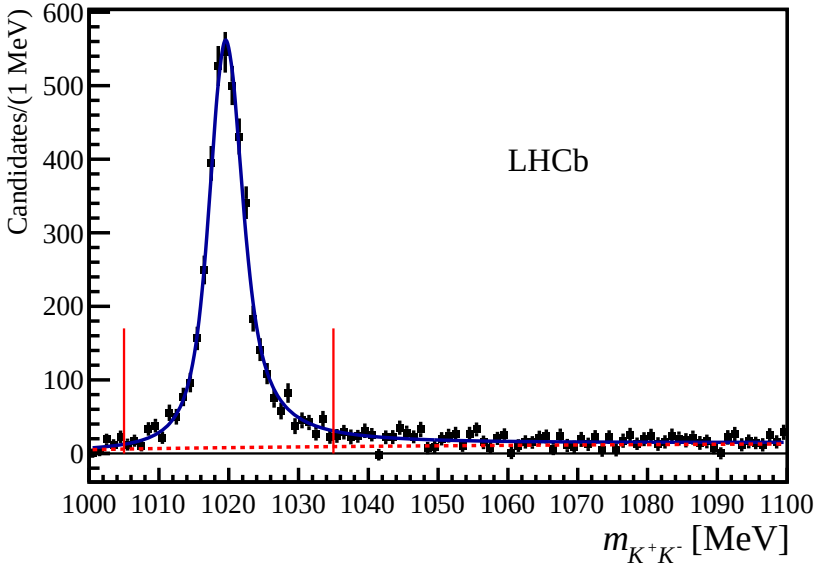

Search for structures in the $J/\psi\,\phi$ spectrum at LHCb

Some analysis details

- Three parametizations: $B^+ \to J/\psi\, K^{*+}$ with $K^{*+} \to \phi K$, $B^+ \to XK^+$ with $X \to J/\psi\,\phi$ and $B^+ \to Z^+\phi$ with $Z^+ \to J/\psi\, K^+$ all followed $J/\psi \to \mu^+\mu^-$ and $\phi \to K^+K^-$.
- Six variables: resonance invariant mass, three helicities angles, and two differences between decay planes.
- Lorentz transformations relates the different helicity representantions.

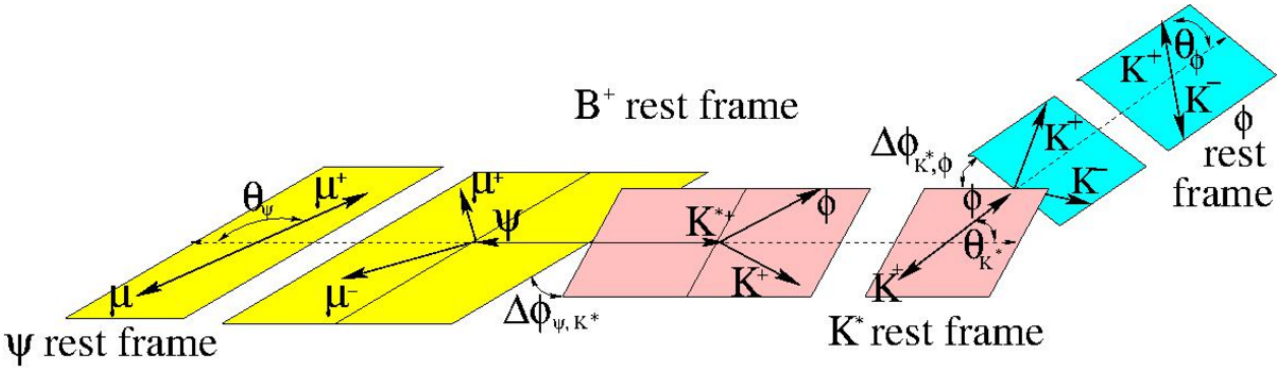

- Resonances described by Breit-Wigner.
- Angular distribution calculated using helicity formalism.

Search for structures in the $J/\psi\,\phi$ spectrum at LHCb

Fit only with conventional contributions

- Using the predictions of the Godfrey-Isgur model as a guide for the K^{*+} quantum numbers [Phys. Rev. D32 (1985) 189.].
- The masses and widths of all states are left free.
- The $m_{\phi K}$ and $m_{J/\psi\,K}$ distributions well with K^{*+} contributions alone.
- The fit projections onto $m_{J/\psi\,\phi}$ do not provide an acceptable description of the data.

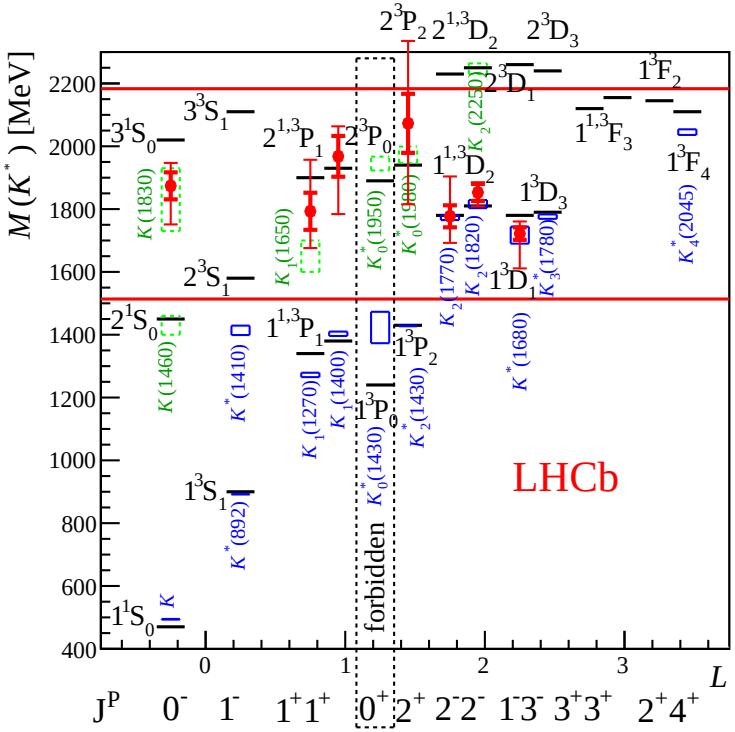

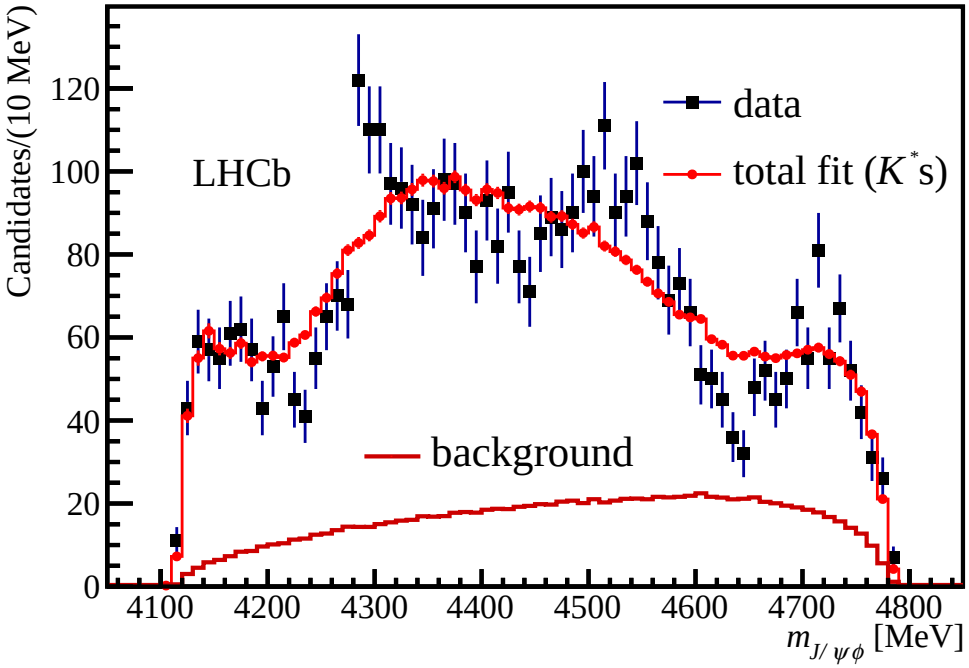

Search for structures in the $J/\psi\,\phi$ spectrum at LHCb

Fit with conventional plus exotic contributions

- Only X contributions lead to significant improvements in the description of the data.
- The model contains seven K^{*+} states, four X states and ϕK and $J/\psi\,\phi$ nonresonant components.

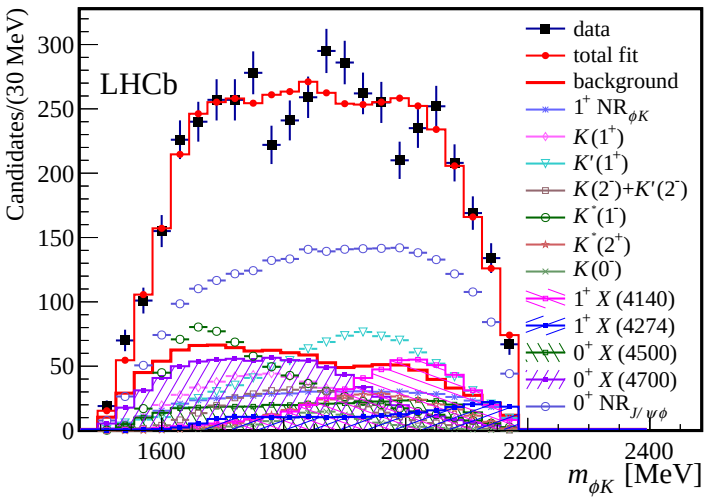

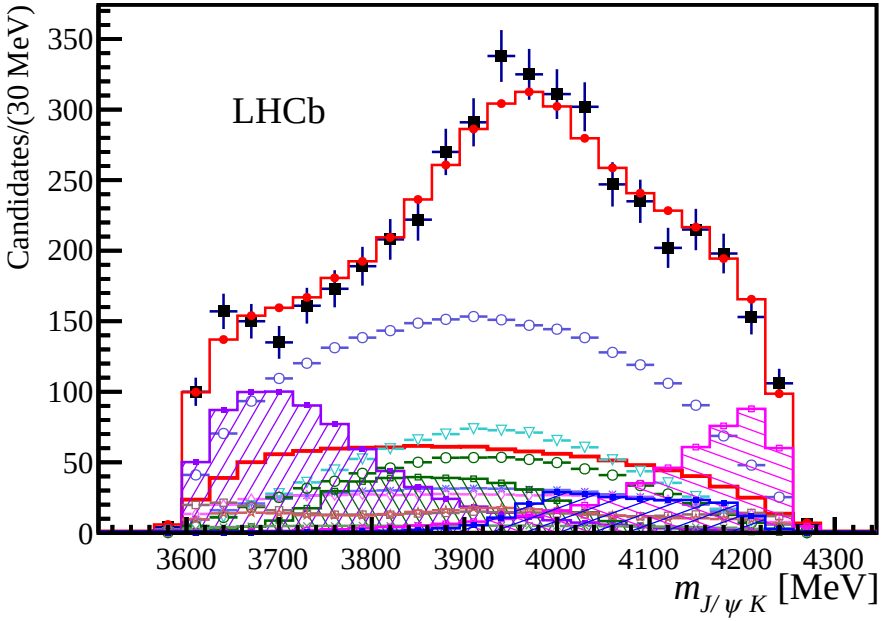

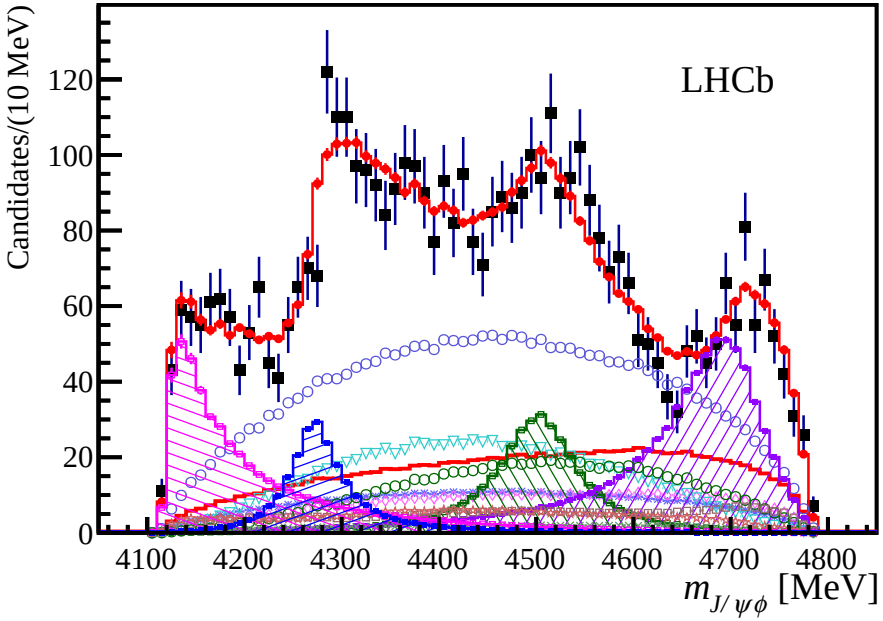

Search for structures in the $J/\psi\,\phi$ spectrum at LHCb

Modeling near threshold X contributions as $D_s^{\pm}\ D_s^{*\mp}$ cusps

- Modeling $X(4140)$ and $X(4274)$ using the threshold cusp parameterization proposed by Swanson [Int. J. Mod. Phys. E, 25, 1642010 (2016)].
- On the left: only $X(4140)$ is represented as a $J^{PC} = 1^{++}\ D_s^{+}\ D_s^{*-}$ cusp.
- On the right: $X(4140)$ and $X(4274)$ are represented as a $J^{PC} = 1^{++}\ D_s^{+}\ D_s^{*-}$ and $J^{PC} = 0^{-+}\ D_s^{\pm} D_s^{*+}(2317)^{\mp}$ cusps, respectively.

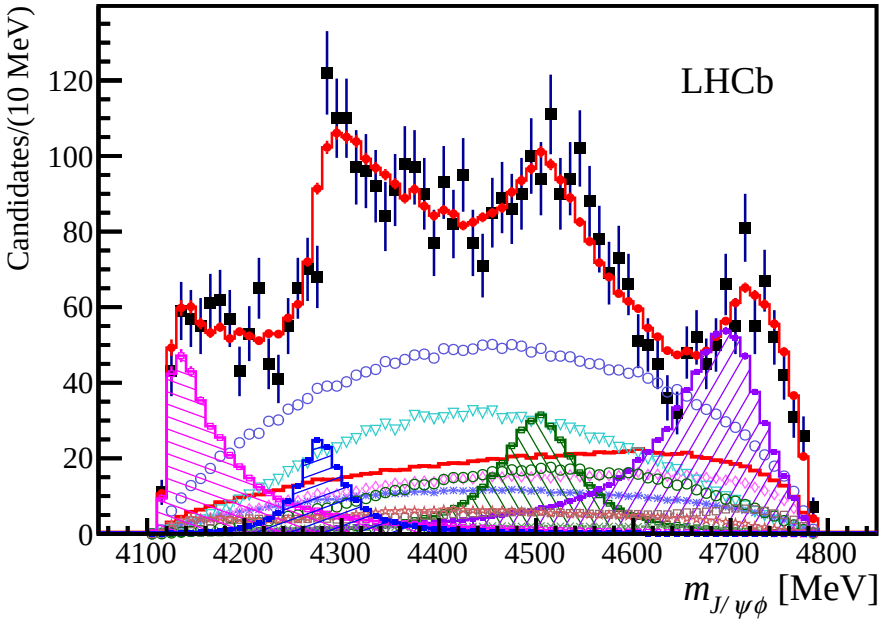

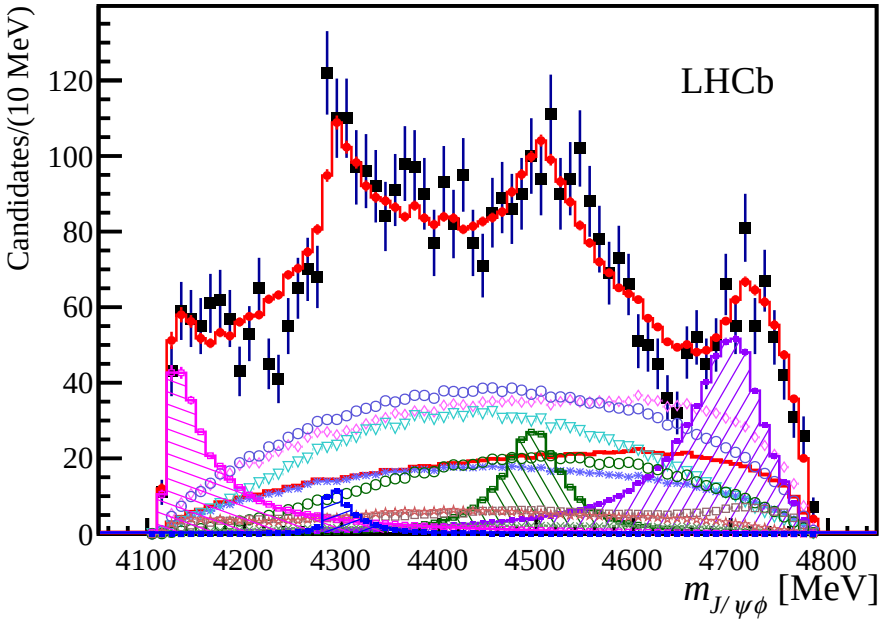

Search for structures in the $J/\psi\,\phi$ spectrum at LHCb

Results

- The LHCb data cannot be well described without several $J/\psi\,\phi$ contributions.

(Table[1] and references [28,25] on arXiv:1606.07895)

Contri-bution	Sign. or Ref.	Fit results M_0 [MeV]	Γ_0 [MeV]	FF %
All $X(1^+)$				$16\pm3\,^{+6}_{-2}$
$X(4140)$	8.4σ	$4146.5\pm4.5\,^{+4.6}_{-2.8}$	$83\pm21\,^{+21}_{-14}$	$13\pm3.2\,^{+4.8}_{-2.0}$
ave.	Table 1	4143.4 ± 1.9	15.7 ± 6.3	
$X(4274)$	6.0σ	$4273.3\pm8.3\,^{+17.2}_{-3.6}$	$56\pm11\,^{+8}_{-11}$	$7.1\pm2.5\,^{+3.5}_{-2.4}$
CDF	28	$4274.4\,^{+8.4}_{-6.7}\pm1.9$	$32\,^{+22}_{-15}\pm8$	
CMS	25	$4313.8\pm5.3\pm7.3$	$38\,^{+30}_{-15}\pm16$	
All $X(0^+)$				$28\pm5\pm7$
$NR_{J/\psi\phi}$	6.4σ			$46\pm11\,^{+11}_{-21}$
$X(4500)$	6.1σ	$4506\pm11\,^{+12}_{-15}$	$92\pm21\,^{+21}_{-20}$	$6.6\pm2.4\,^{+3.5}_{-2.3}$
$X(4700)$	5.6σ	$4704\pm10\,^{+14}_{-24}$	$120\pm31\,^{+42}_{-33}$	$12\pm5\,^{+9}_{-5}$

- X contributions near threshold are consistent with $D_s^{\pm}\ D_s^{*\mp}$ cusps.
- First full amplitude analysis performed on $B^{\pm}\to J/\psi\,\phi K^{\pm}$ decays.

Charmonium-like exotic states spectroscopy at LHC

Recent results not included in this talk

LHCb:

- **$Z(4430)^+$: model independent analysis** [Phys. Rev. D 92, 112009 (2015)].
- **Confirmation of $Z(4430)^+$ at LHCb** [Phys.Rev.Lett.112, 222002 (2014)].
- **$\mathrm{X}(3872)$ quantum numbers determination** [Phys. Rev. Lett. 110, 222001 (2013)].
- **Evidence of $\mathrm{X}(3872) \to \psi(2S)\gamma$** [Nuclear Physics B 886 (2014) 665-680].
- **Quantum numbers of the $\mathrm{X}(3872)$ state and orbital angular momentum in its $\rho^0 J/\psi$ decays** [Phys. Rev. D 92 (2015) 011102].

ATLAS:

- **Production measurements of $\psi(2S)$ and $\mathrm{X}(3872)$ in pp collisions at 8 TeV** [ATLAS-CONF-2016-028].

Many other results in b and c spectroscopy

Access: http://lhcbproject.web.cern.ch/lhcbproject/Publications/LHCbProjectPublic/Summary_all.html

The LHCb Public results

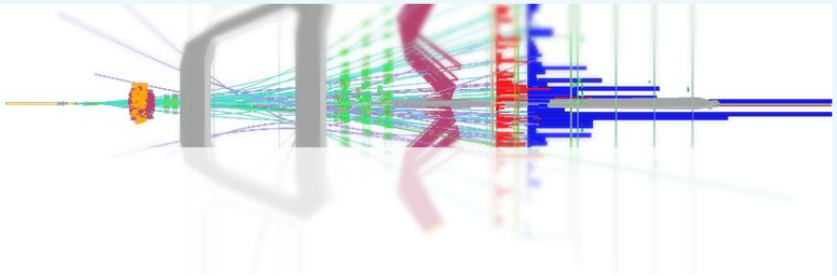

LHCb publications

[to restricted-access page]

PUBLICATIONS PER WORKING GROUP

- FLAVOUR TAGGING
- b-HADRONS AND QUARKONIA
- B DECAYS TO CHARMONIUM
- DETECTOR PERFORMANCE
- CHARMLESS b-HADRON DECAYS
- QCD, ELECTROWEAK AND EXOTICA
- RARE DECAYS
- CHARM PHYSICS
- SEMILEPTONIC B DECAYS
- LUMINOSITY
- B DECAYS TO OPEN CHARM

List of papers (Total of 284 papers)

TITLE	DOCUMENT NUMBER	JOURNAL	SUBMITTED ON
Search for the rare decays $B^0 \to J/\psi\gamma$ and $B_s^0 \to J/\psi\gamma$	PAPER-2015-044	PRD	16 Oct 2015
Evidence for the strangeness-changing weak decay $\Xi_b^- \to \Lambda_b^0\pi^-$	PAPER-2015-047	PRL	13 Oct 2015
A model-independent confirmation of the $Z(4430)^-$ state	PAPER-2015-038	PRD	07 Oct 2015
Measurements of prompt charm production cross-sections in pp collisions at $\sqrt{s} = 13\mathrm{TeV}$	PAPER-2015-041	JHEP	06 Oct 2015
Model-independent measurement of mixing parameters in $D^0 \to K_S\pi^+\pi^-$ decays	PAPER-2015-042	JHEP	06 Oct 2015
Measurement of the forward-backward asymmetry in $Z/\gamma^* \to \mu^+\mu^-$ decays and determination of the effective weak mixing angle	PAPER-2015-039	JHEP	25 Sep 2015
Studies of the resonance structure in $D^0 \to K_S^0K^\pm\pi^\mp$ decays	PAPER-2015-026	PRD	22 Sep 2015
Forward production of Υ mesons in pp collisions at $\sqrt{s} = 7$ and 8TeV	PAPER-2015-045	JHEP	08 Sep 2015
Measurement of forward J/ψ production cross-sections in pp collisions at $\sqrt{s} = 13$ TeV	PAPER-2015-037	JHEP	02 Sep 2015
First measurement of the differential branching fraction and CP asymmetry of the $B^\pm \to \pi^\pm\mu^+\mu^-$ decay	PAPER-2015-035	JHEP	01 Sep 2015
Measurement of CP violation parameters and polarisation fractions in $B_s^0 \to J/\psi\overline{K}^{*0}$ decays	PAPER-2015-034	JHEP	01 Sep 2015
Study of the production of Λ_b^0 and $\overline{B}^0$ hadrons in pp collisions and first measurement of the $\Lambda_b^0 \to J/\psi pK^-$ branching fraction	PAPER-2015-032	Chin Phys C	01 Sep 2015
Measurement of the time-integrated CP asymmetry in $D^0 \to K_S^0K_S^0$ decays	PAPER-2015-030	JHEP	25 Aug 2015
Search for hidden-sector bosons in $B^0 \to K^{*0}\mu^+\mu^-$ decays	PAPER-2015-036	PRL	17 Aug 2015
Measurement of the $B_s^0 \to \phi\phi$ branching fraction and search for the decay $B^0 \to \phi\phi$	PAPER-2015-028	JHEP	04 Aug 2015
B flavour tagging using charm decays at the LHCb experiment	PAPER-2015-027	JINST	28 Jul 2015
Measurement of the branching fraction ratio $\mathcal{B}(B_c^+ \to \psi(2S)\pi^+)/\mathcal{B}(B_c^+ \to J/\psi\pi^+)$	PAPER-2015-024	PRD	13 Jul 2015
Observation of $J/\psi p$ resonances consistent with pentaquark states in $\Lambda_b^0 \to J/\psi K^-p$ decays	PAPER-2015-029	Phys. Rev. Lett. 115 (2015) 072001	13 Jul 2015
Search for long-lived heavy charged particles using a ring imaging Cherenkov technique at LHCb	PAPER-2015-002	JHEP	30 Jun 2015
Angular analysis and differential branching fraction of the decay $B_s^0 \to \phi\mu^+\mu^-$	PAPER-2015-023	JHEP	29 Jun 2015

Summary

Pentaquark states in $\Lambda_b^0 \to J/\psi\, p K^-$ at LHCb

- $P(4380)_c^+$ observed with 9.0σ in multidimensional amplitude fit. Quantum numbers $J^P = 3/2^-$.
- $P(4450)_c^+$ observed with 12.0σ in multidimensional amplitude fit. Quantum numbers $J^P = 5/2^+$.
- Resonance behavior observed for $P(4450)_c^+$. $P(4380)_c^+$ needs further studies.
- Model independent analysis rules out conventional only explanation with 9σ.

Evidence for exotic hadron contributions to $\Lambda_b^0 \to J/\psi\, p \pi^-$ at LHCb

- Evidence of exotic contributions observed with 3.1σ .
- $P(4380)_c^+$: $(5.1 \pm 1.5^{+2.6}_{-1.6})\%$
- $P(4450)_c^+$: $(1.6^{+0.8}_{-0.6}{}^{+0.6}_{-0.5})\%$
- $Z_c(4200)^+$: $(7.7 \pm 2.8^{+3.4}_{-4.0})\%$

Summary

Search for structures in the $J/\psi\,\phi$ spectrum at LHCb and CMS

- First full amplitude analysis performed on $B^{\pm} \to J/\psi\,\phi K^{\pm}$ with $J/\psi \to \mu^{+}\mu^{-}$ and $\phi \to K^{+}K^{-}$.
- $X(4140)$ and $X(4274)$ resonances confirmed with consistent masses and larger widths than previous measurements.
- Two new higher mass resonances observed with high significance.
- $X(4140)$ and $X(4274)$ contributions also consistent with $D_s^{\pm}\ D_s^{*\mp}$ cusps.

Thanks!

Backup

$\Lambda_b^0 \to K^- p J/\psi$

Fit results without pentaquark states

- Fit including only Λ^* resonances, allowing all possible known states (Extended model)
- The masses and widths of the Λ^* states are fixed to their PDG values
- The m_{Kp} distribution is reasonably well fitted
- The peaking structure in $m_{J/\psi\, p}$ is not described

State	J^P	M_0 (MeV)	Γ_0 (MeV)	# Reduced	# Extended
$\Lambda(1405)$	$1/2^-$	$1405.1^{+1.3}_{-1.0}$	50.5 ± 2.0	3	4
$\Lambda(1520)$	$3/2^-$	1519.5 ± 1.0	15.6 ± 1.0	5	6
$\Lambda(1600)$	$1/2^+$	1600	150	3	4
$\Lambda(1670)$	$1/2^-$	1670	35	3	4
$\Lambda(1690)$	$3/2^-$	1690	60	5	6
$\Lambda(1800)$	$1/2^-$	1800	300	4	4
$\Lambda(1810)$	$1/2^+$	1810	150	3	4
$\Lambda(1820)$	$5/2^+$	1820	80	1	6
$\Lambda(1830)$	$5/2^-$	1830	95	1	6
$\Lambda(1890)$	$3/2^+$	1890	100	3	6
$\Lambda(2100)$	$7/2^-$	2100	200	1	6
$\Lambda(2110)$	$5/2^+$	2110	200	1	6
$\Lambda(2350)$	$9/2^+$	2350	150	0	6
$\Lambda(2585)$	?	$\approx$2585	200	0	6

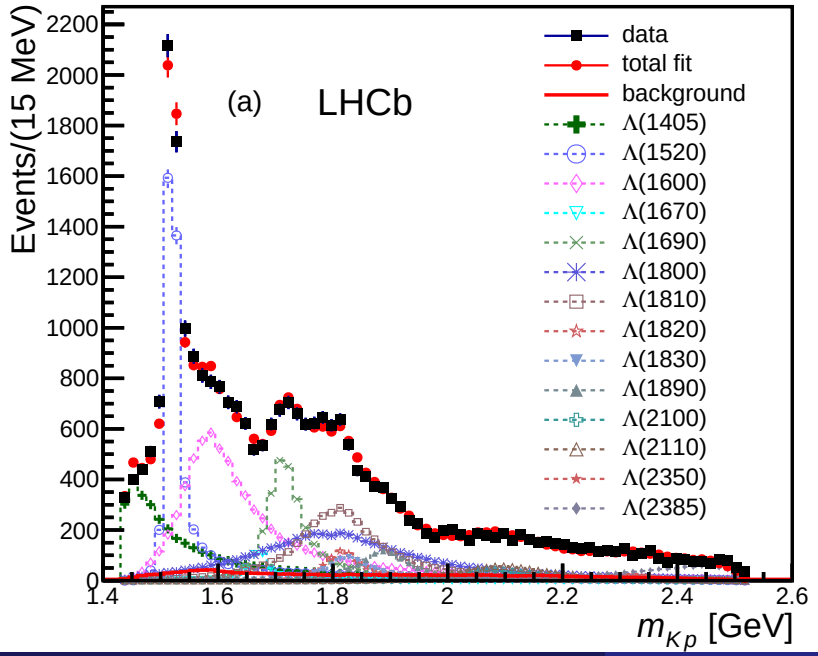

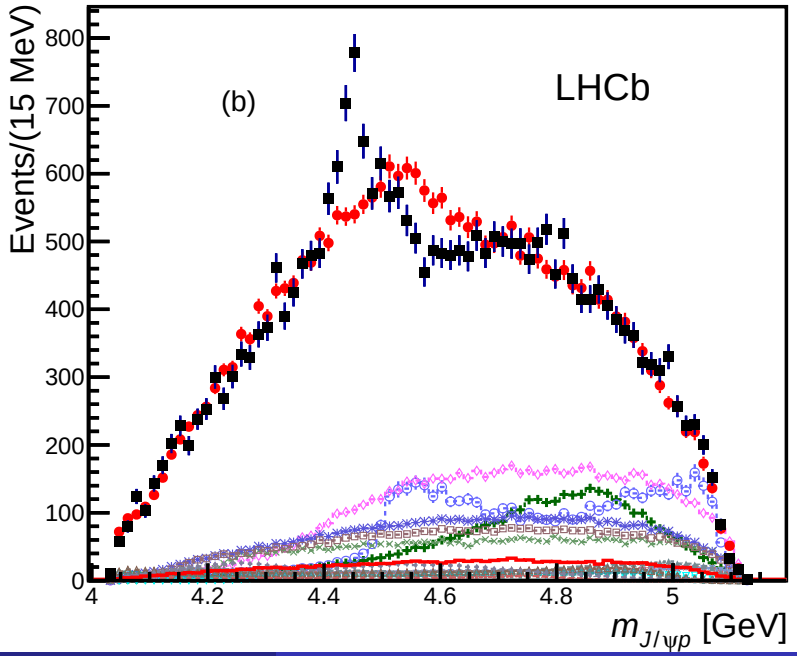

$\Lambda_b^0 \to K^- p J/\psi$: Systematic uncertainties

Table 2: Summary of systematic uncertainties on P_c^+ masses, widths and fit fractions, and Λ^* fit fractions. A fit fraction is the ratio of the phase space integrals of the matrix element squared for a single resonance and for the total amplitude. The terms "low" and "high" correspond to the lower and higher mass P_c^+ states. The sFit/cFit difference is listed as a cross-check and not included as an uncertainty.

Source	M_0 (MeV)		Γ_0 (MeV)		Fit fractions (%)			
	low	high	low	high	low	high	$\Lambda(1405)$	$\Lambda(1520)$
Extended vs. reduced	21	0.2	54	10	3.14	0.32	1.37	0.15
Λ^* masses & widths	7	0.7	20	4	0.58	0.37	2.49	2.45
Proton ID	2	0.3	1	2	0.27	0.14	0.20	0.05
$10 < p_p < 100$ GeV	0	1.2	1	1	0.09	0.03	0.31	0.01
Nonresonant	3	0.3	34	2	2.35	0.13	3.28	0.39
Separate sidebands	0	0	5	0	0.24	0.14	0.02	0.03
J^P $(3/2^+, 5/2^-)$ or $(5/2^+, 3/2^-)$	10	1.2	34	10	0.76	0.44		
$d = 1.5 - 4.5$ GeV^{-1}	9	0.6	19	3	0.29	0.42	0.36	1.91
$L_{\Lambda_b^0}^{P_c}$ $\Lambda_b^0 \to P_c^+$ (low/high)K^-	6	0.7	4	8	0.37	0.16		
L_{P_c} P_c^+ (low/high) $\to J/\psi p$	4	0.4	31	7	0.63	0.37		
$L_{\Lambda_b^0}^{\Lambda_n^*}$ $\Lambda_b^0 \to J/\psi \Lambda^*$	11	0.3	20	2	0.81	0.53	3.34	2.31
Efficiencies	1	0.4	4	0	0.13	0.02	0.26	0.23
Change $\Lambda(1405)$ coupling	0	0	0	0	0	0	1.90	0
Overall	29	2.5	86	19	4.21	1.05	5.82	3.89
sFit/cFit cross check	5	1.0	11	3	0.46	0.01	0.45	0.13

$\Lambda_b^0 \to K^- p J/\psi$: Slices $m_{pJ/\psi}$

Figure 8: $m_{J/\psi p}$ in various intervals of m_{Kp} for the fit with two P_c^+ states: (a) $m_{Kp} < 1.55$ GeV, (b) $1.55 < m_{Kp} < 1.70$ GeV, (c) $1.70 < m_{Kp} < 2.00$ GeV, and (d) $m_{Kp} > 2.00$ GeV. The data are shown as (black) squares with error bars, while the (red) circles show the results of the fit. The blue and purple histograms show the two P_c^+ states. See Fig. 7 for the legend.

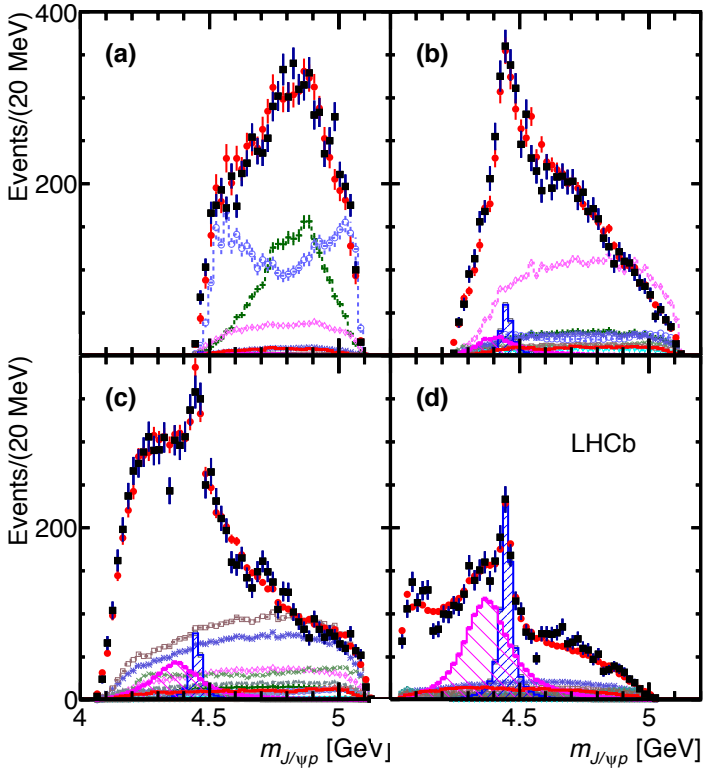

$\Lambda_b^0 \to K^- p J/\psi$: Slices $m_{KJ/\psi}$

Figure 11: Projections onto $m_{J/\psi K}$ in various intervals of m_{Kp} for the reduced model fit (cFit) with two P_c^+ states of J^P equal to $3/2^-$ and $5/2^+$: (a) $m_{Kp} < 1.55$ GeV, (b) $1.55 < m_{Kp} < 1.70$ GeV, (c) $1.70 < m_{Kp} < 2.00$ GeV, (d) $m_{Kp} > 2.00$ GeV, and (e) all m_{Kp}. The data are shown as (black) squares with error bars, while the (red) circles show the results of the fit. The individual resonances are given in the legend.

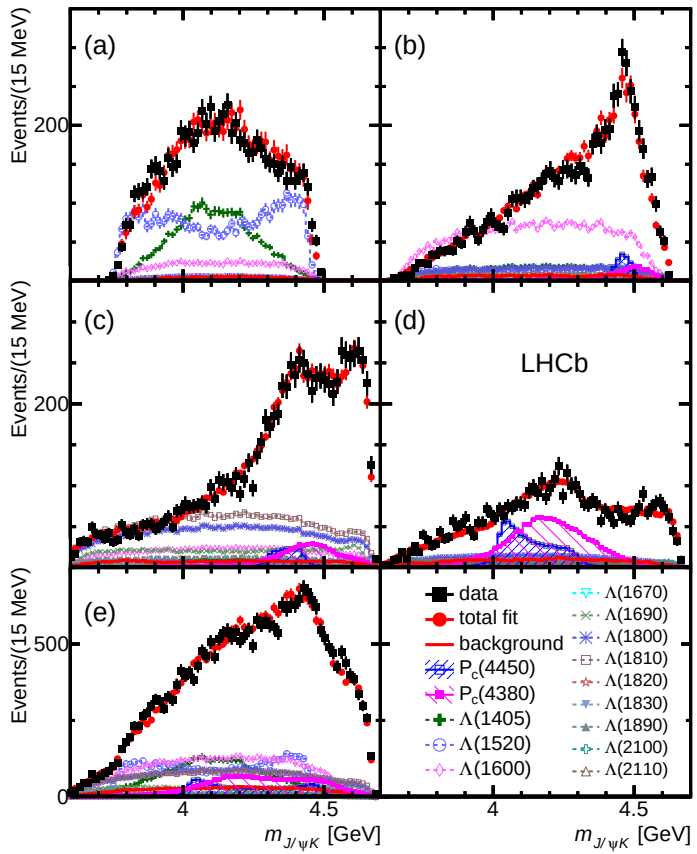

$Z(4430)^+$

- Charged charmonium like state reported by Belle in $B^0 \to \psi(2S)K^+\pi^-$ decays [Phys.Rev.D88:074026]
- Searched and not confirmed or excluded by BaBar [Phys.Rev.D79:112001]
- Can not be explained as conventional meson.
- Minimum quark content: $c\bar{c}u\bar{d}$
- No corresponding structure observed in $B^0 \to J/\psi K^+\pi^-$

$Z(4430)^+$ at Belle. K^{*0} and $K_2^*(1432)$ vetoed.

With $Z(4430)^+$ and No $Z(4430)^+$

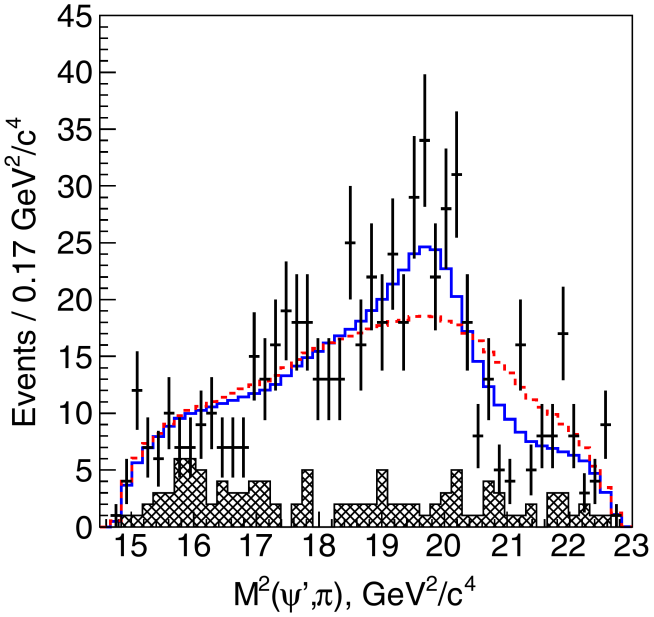

$Z(4430)^+$ at BaBar. Legendre polynomials approach.

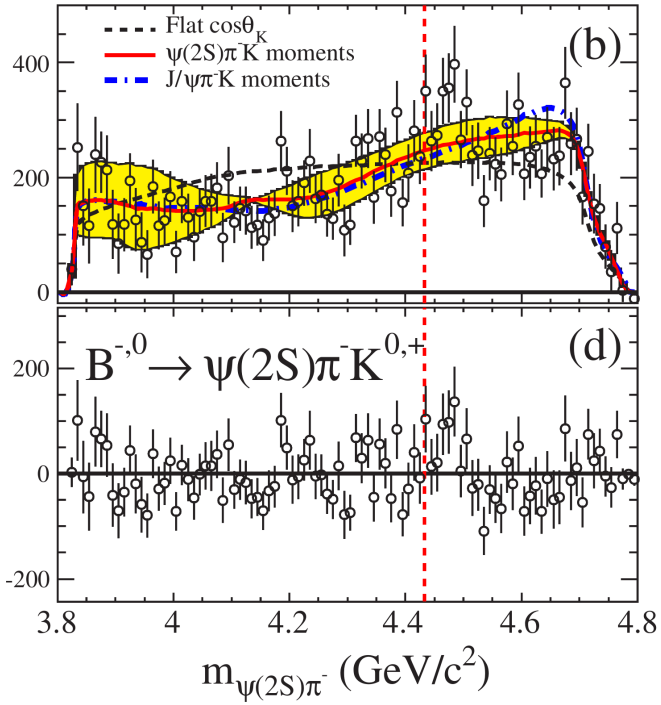

$Z(4430)^+$: model independent analysis

Phys. Rev. D 92, 112009 (2015)

The main goal is to check if the structures in the $\mathrm{m}_{\psi(2S)\pi}$ spectrum can be explained as reflections of the resonance activity in the $\mathrm{K}\pi$ system.

- No assumptions on the shape and coupling of the K^* resonances.
- Only its maximum J is restricted.

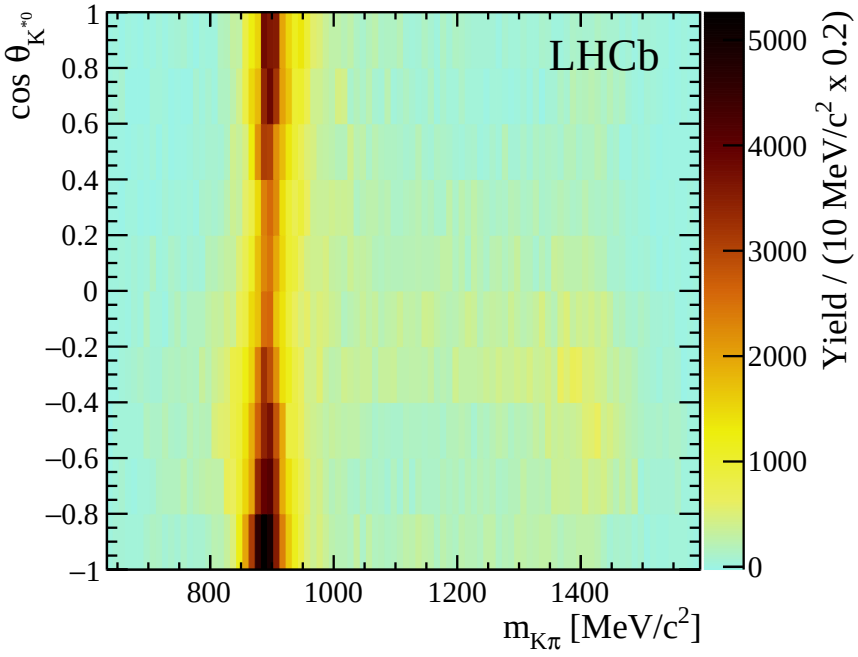

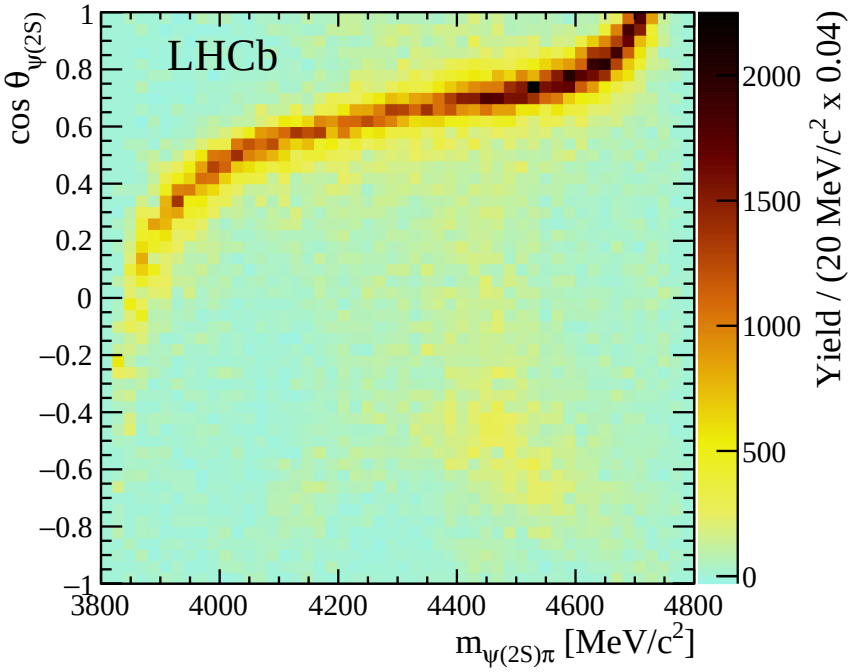

$Z(4430)^+$: model independent analysis

Slices of $m_{K\pi}$

Toy Monte Carlo prediction in slices of $m_{K\pi}$.

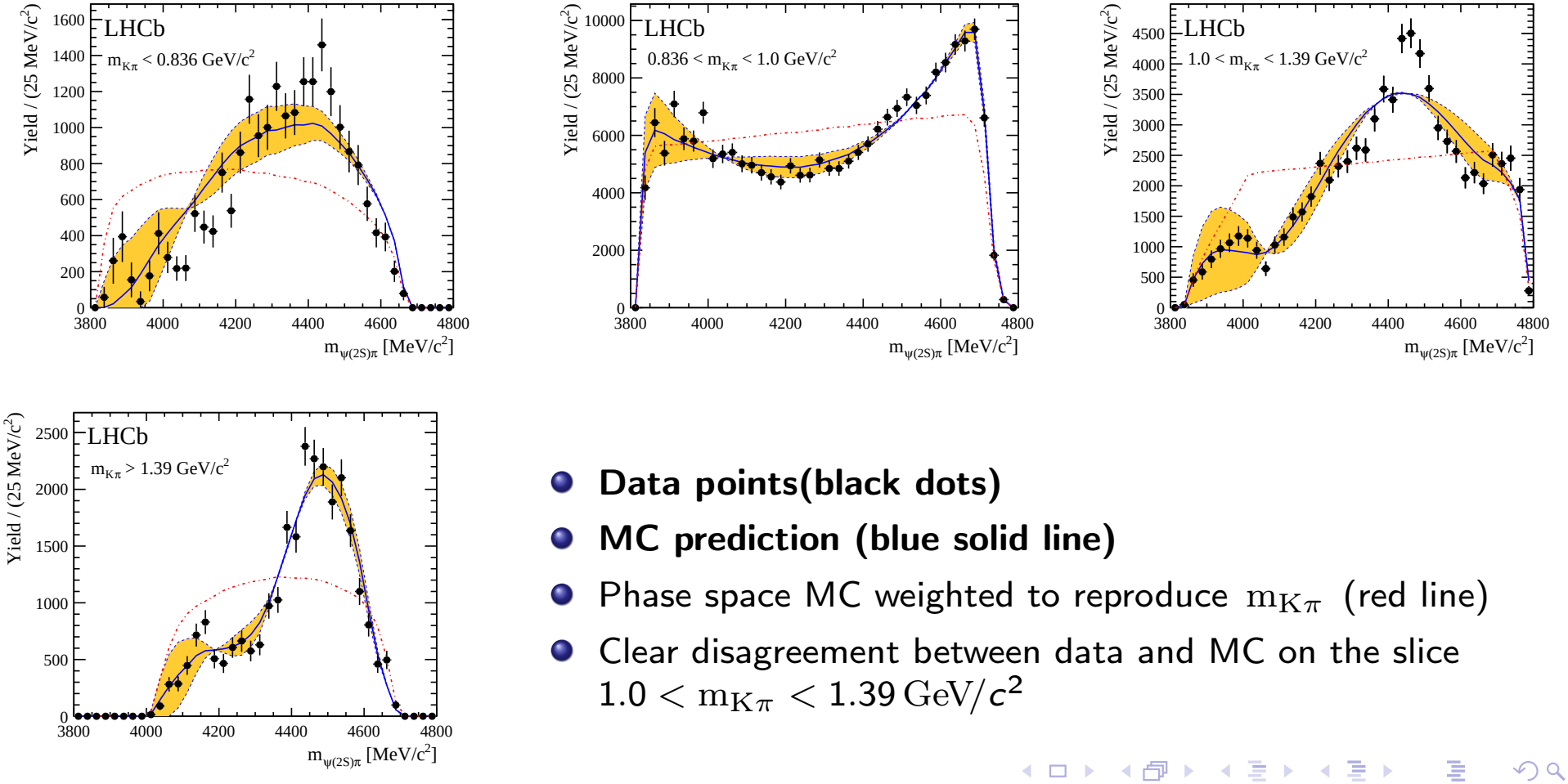

- **Data points(black dots)**
- **MC prediction (blue solid line)**
- Phase space MC weighted to reproduce $m_{K\pi}$ (red line)
- Clear disagreement between data and MC on the slice $1.0 < m_{K\pi} < 1.39\,\mathrm{GeV}/c^2$

$Z(4430)^+$: model independent analysis

Additional studies: $l_{max} \leq 4$

- Setting the maximum Legendre polynomial order to four, independent of $m_{K\pi}$
- This corresponds to suppose the $K\pi$ system has S,P and D waves contributing in all regions.
- Data can not be reproduced

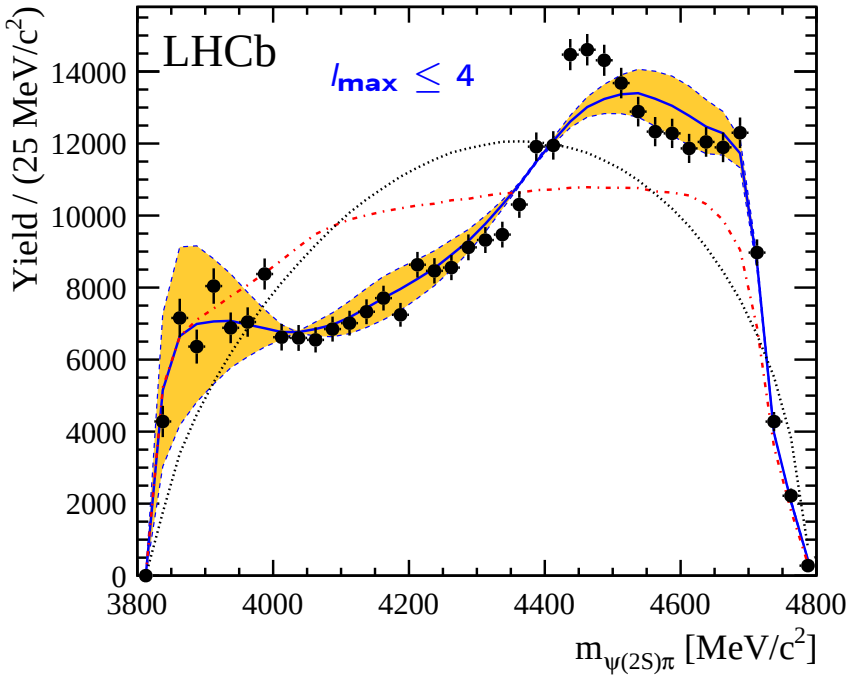

full $m_{K\pi}$ spectrum

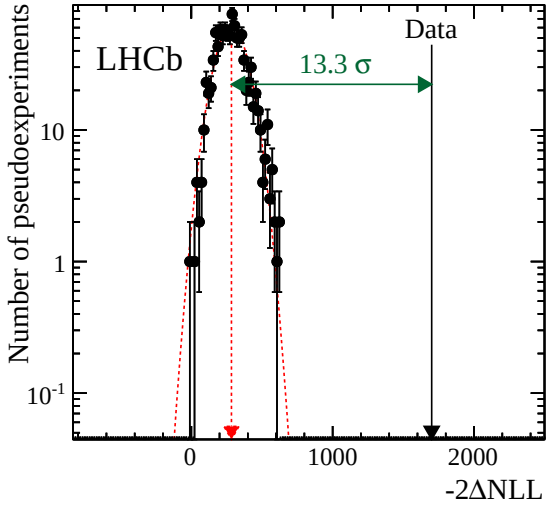

$1.0 < m_{K\pi} < 1.39\ \mathrm{GeV}/c^2$

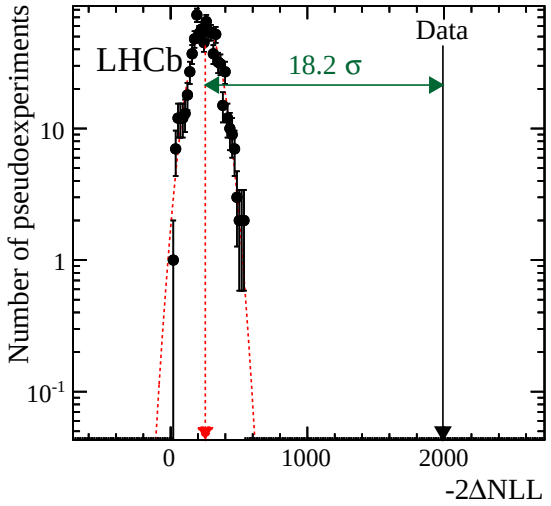

$Z(4430)^+$: model independent analysis

Additional studies: $l_{max} \leq 6$

- Setting the maximum Legendre polynomial order to six, independent of $m_{K\pi}$
- This corresponds to suppose the $K\pi$ system has S, P, D and F waves contributing in all regions.
- Data still can not be reproduced

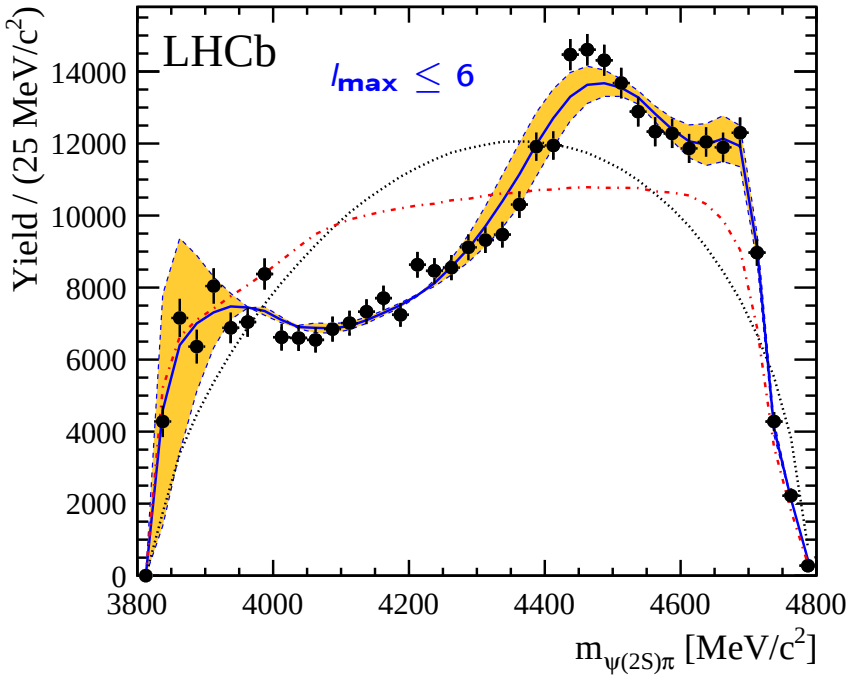

full $m_{K\pi}$ spectrum

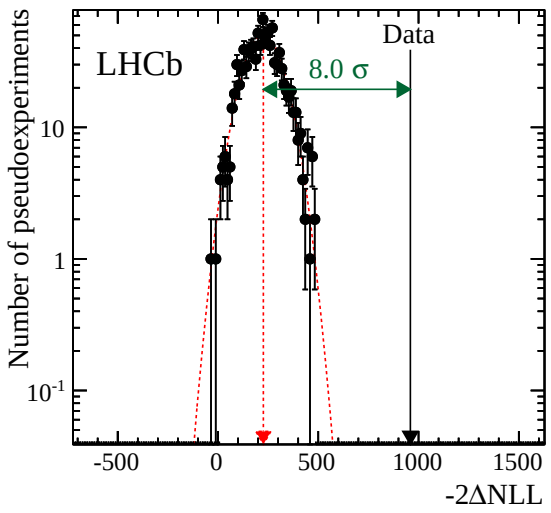

$1.0 < m_{K\pi} < 1.39\ \mathrm{GeV}/c^2$

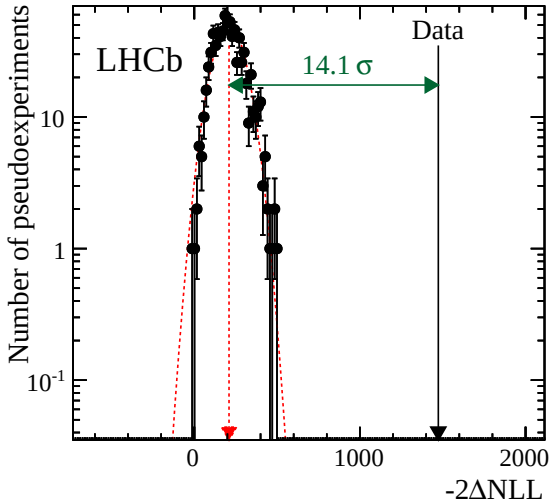

Confirmation of $Z(4430)^+$ at LHCb

Phys.Rev.Lett.112, 222002 (2014)

- Sample with >25.000 $B^0 \to K^+\pi^-\psi(2S)$ signal candidates,
- Analysis performed using two different approaches:
  - Model dependent. Four-dimensional amplitude fit (invariant masses, helicity and decay planes angles).
  - Model independent. An analysis based on the Legendre polynomial moments extracted from the $K\pi$ system
- Background from sidebands. Estimated 4% of combinatorial background in the signal region.
- Four-dimensional efficiency calculated using complete simulation of the detector

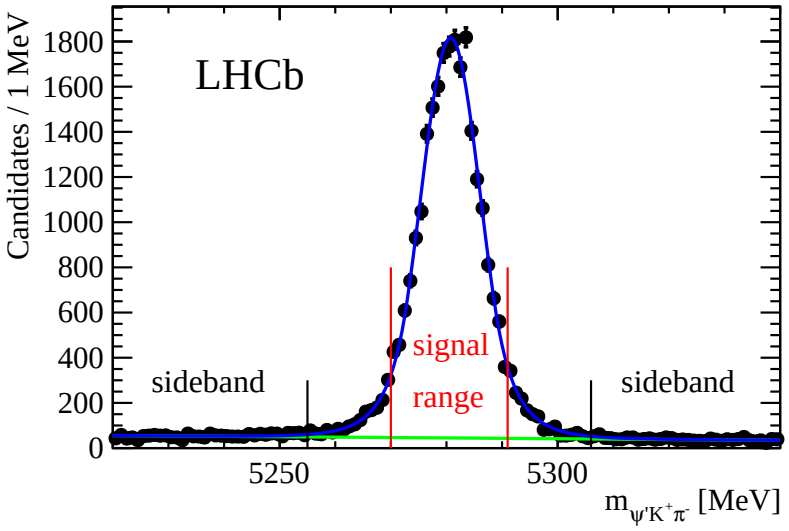

background subtracted Dalitz plot

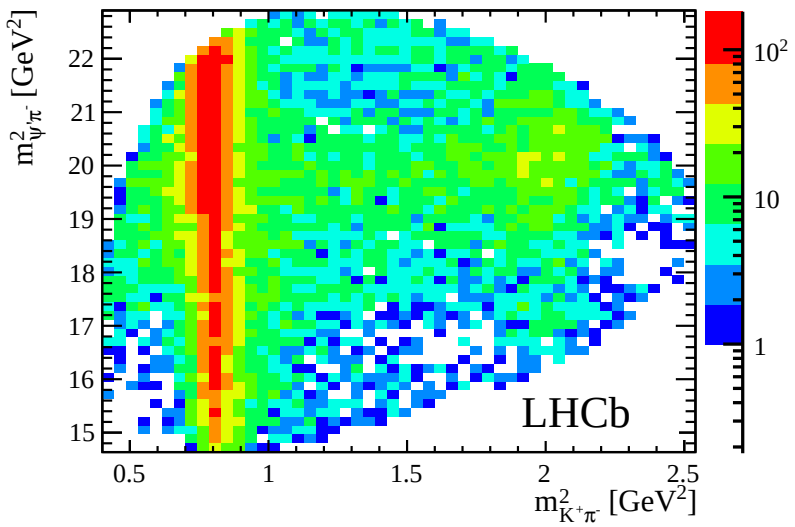

$Z(4430)^+$
Amplitude fit

- Fitted parameters:

$$M_{Z(4430)^+} = 4475 \pm 7^{+15}_{-25}\,\mathrm{MeV}/c^2, \Gamma_{Z(4430)^+} = 172 \pm 13^{+37}_{-34}\,\mathrm{MeV}/c^2$$

$$f_{Z(4430)^+} = (5.9 \pm 0.9^{+1.5}_{-3.3})\%$$

.

- Significance: $\Delta(-2lnL) > 13.9\sigma$

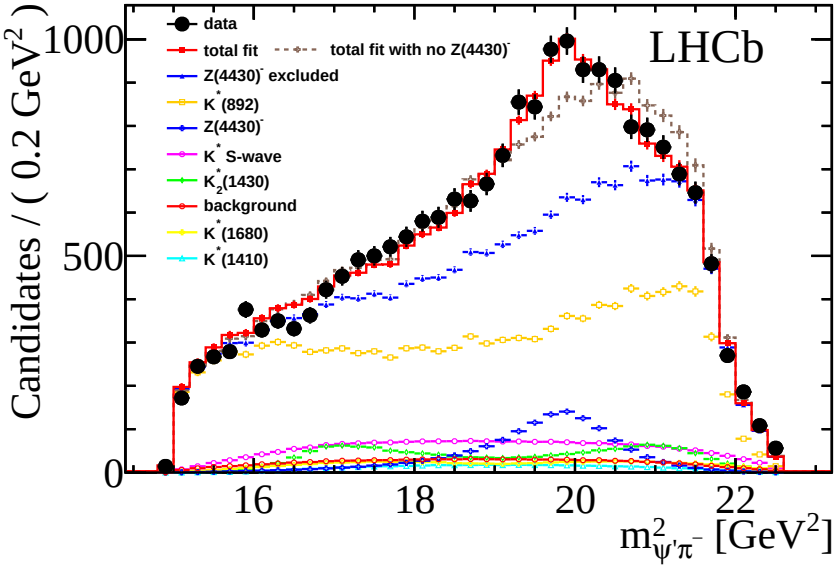

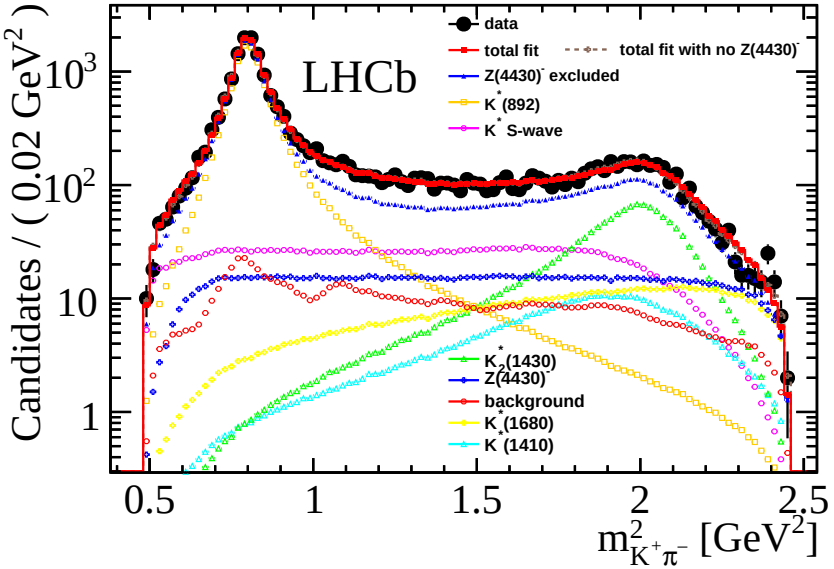

$Z(4430)^+$

Resonance character and spin determination

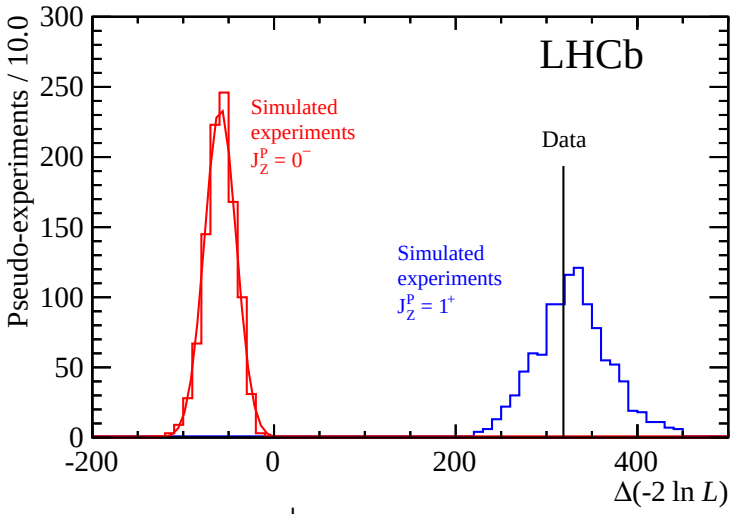

- $J^P = 1^+$ assignment favored.
- Other J^P assignments are ruled out with large significance: $> 9\sigma$

- $Z(4430)^+$ amplitude is described by 6 independent complex numbers instead of a Breit-Wigner
- Observe a fast change of phase crossing maximum of magnitude.
- Expected behaviour for a resonance.

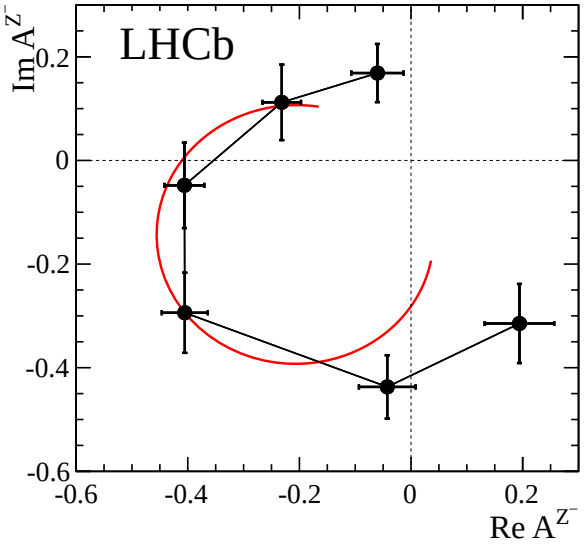

$Z(4430)^+$: model independent analysis

Phys. Rev. D 92, 112009 (2015)

- Very active $\mathrm{K}\pi$ system.
- $\mathrm{m}_{\mathrm{K}\pi}$ taken directly from data, as it is.
- Angular structure of the $\mathrm{K}\pi$ system acquired via Legendre polynomials.
- $\frac{dN}{d\cos\theta_{K^*0}} = \sum_{j=0}^{l_{\mathbf{max}}} \langle P_j^U \rangle \mathrm{P}_j(\cos\theta_{K^*0})$
- $\langle P_j^U \rangle = \sum_{i=1}^{N_{\mathbf{reco}}} \frac{W^i_{\mathbf{signal}}}{\epsilon^i} \mathrm{P}_j(\cos\theta^i_{K^*0})$

Resonance	Mass (MeV/c^2)	Γ (MeV/c^2)	J^P
$K^*(800)^0$	682±29	547±24	0^+
$K^*(892)^0$	895.81±0.19	47.4±0.6	1^-
$K^*(1410)^0$	1414±15	232±21	1^-
$K_0^*(1430)^0$	1425±50	270±80	0^+
$K_2^*(1430)^0$	1432.4±1.3	109±5	2^+
$K^*(1680)^0$	1717±27	322±110	1^-
$K_3^*(1780)^0$	1776±7	159±21	3^-

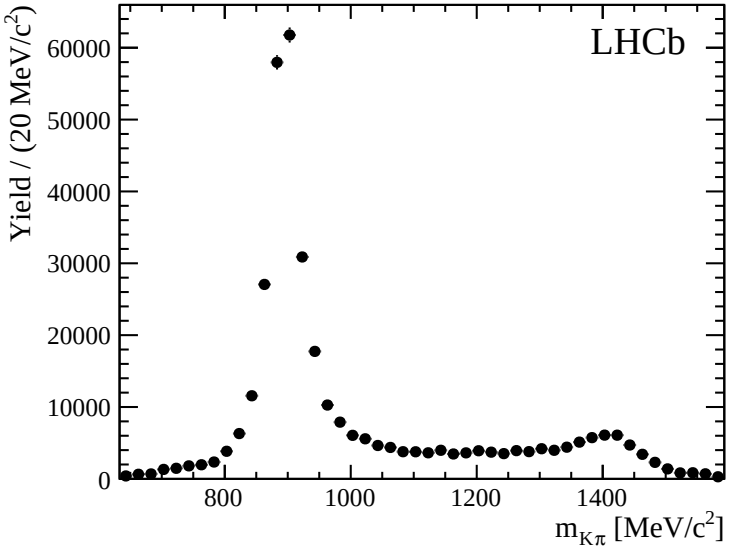

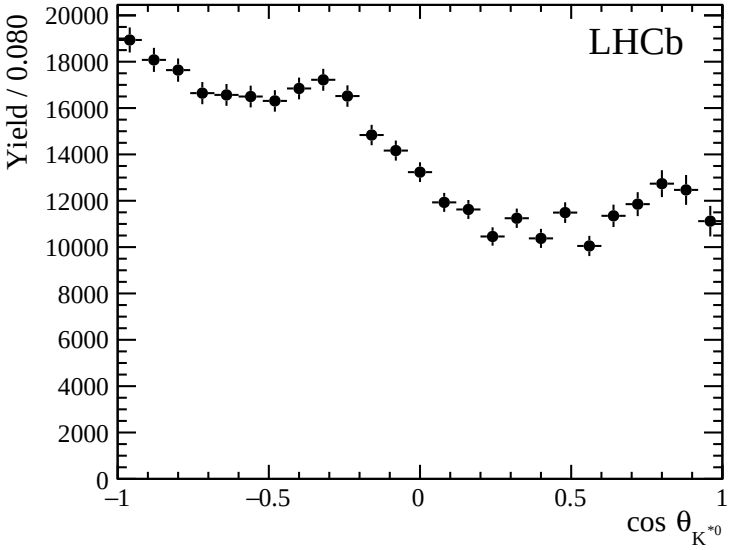

$Z(4430)^+$: model independent analysis

Legendre polynomial moments

The rich angular structure of the $K\pi$ system is shown by the very featured Legendre polynomial moments.

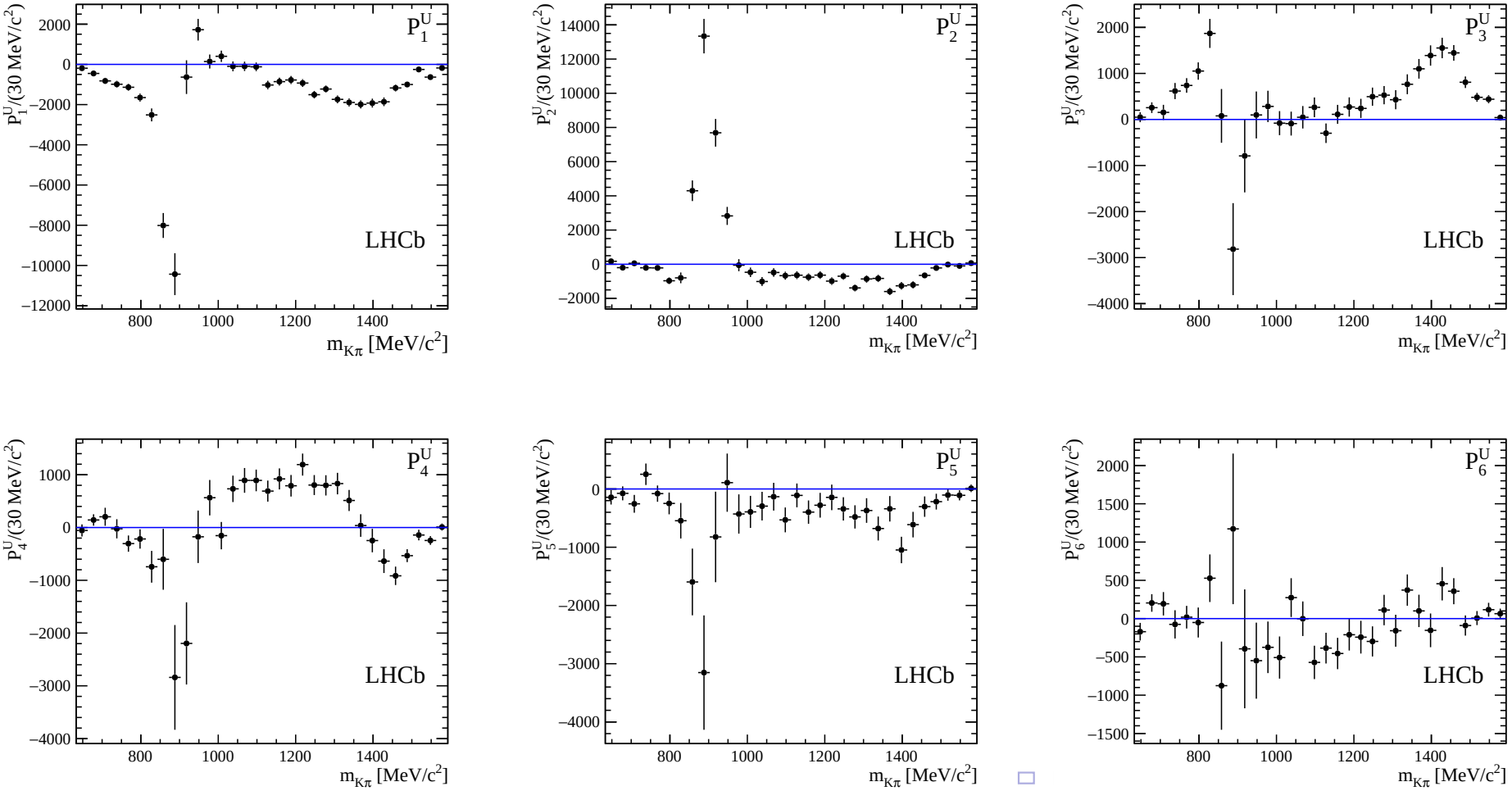

$Z(4430)^+$: model independent analysis

$m_{\psi(2S)\pi}$ spectrum

- The moments are normalized and used to predict, through a MC simulation, the expected $m_{\psi(2S)\pi}$ spectrum.
- The order of the Legendre polynomial expansion depends on the locally dominant $K\pi$ resonances

$$l_{\text{max}}(m_{K\pi}) = \begin{cases} 2 & m_{K\pi} < 836\,\text{MeV}/c^2 \\ 3 & 836\,\text{MeV}/c^2 < m_{K\pi} < 1000\,\text{MeV}/c^2 \\ 4 & m_{K\pi} > 1000\,\text{MeV}/c^2. \end{cases}$$

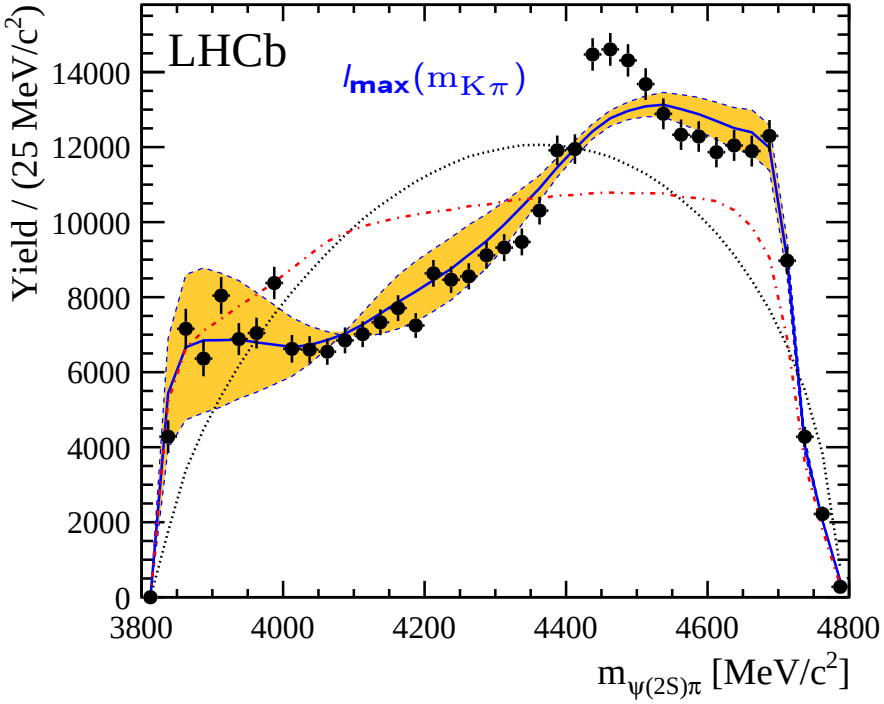

- **Data points(black dots)**
- **MC prediction (blue solid line)**
- Phase space MC (black dotted line)
- Phase space MC weighted to reproduce $m_{K\pi}$ (red line)

$Z(4430)^+$: model independent analysis

Hypothesis test

- Performed using a series of pseudo-experiments produced according with l_{max} ($\mathrm{m_{K\pi}}$).
- Hypothesis test based on likelihood ratio between l_{max} ($\mathrm{m_{K\pi}}$) and l_{max} =30.
- Efficiency effects and background subtraction taken into account in the pseudo-experiment generation.

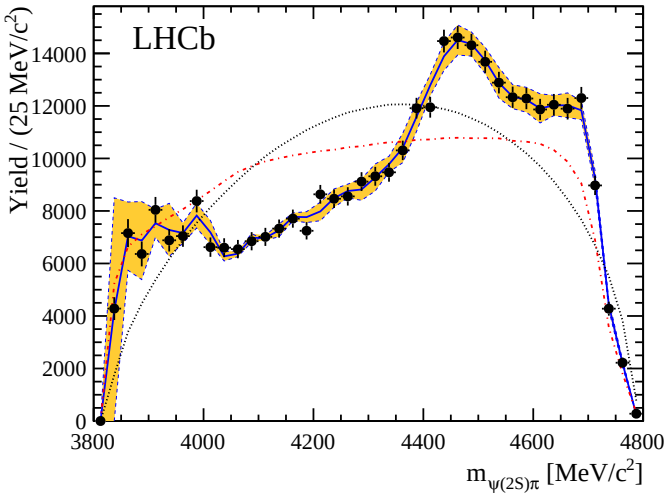

full $\mathrm{m_{K\pi}}$ spectrum

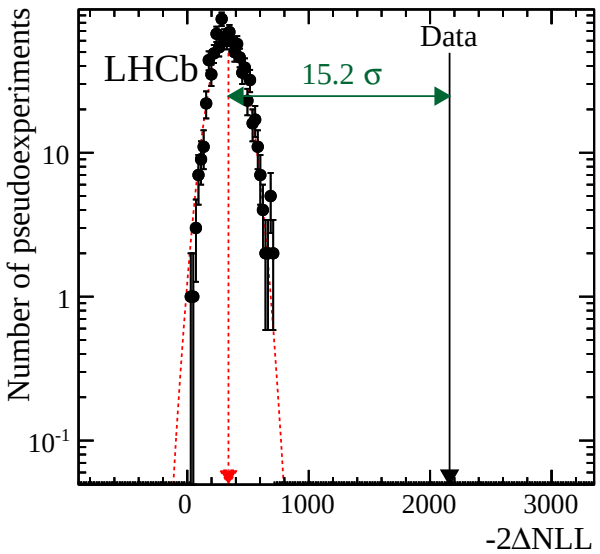

$1.0 < \mathrm{m_{K\pi}} < 1.39\,\mathrm{GeV}/c^2$

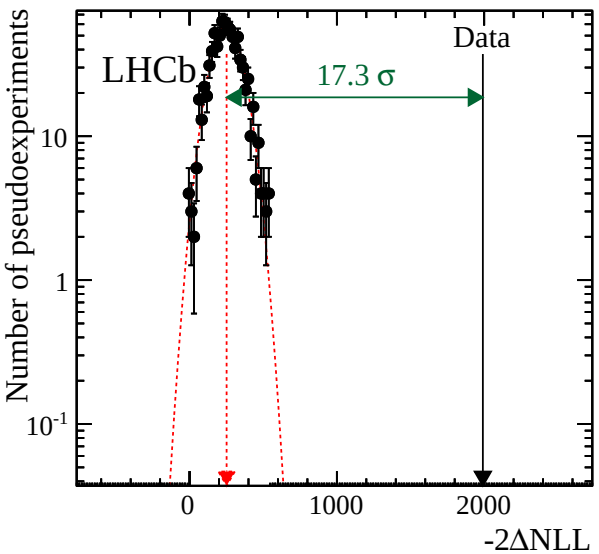

The hypotesis that the structure of the $\mathrm{m_{\psi(2S)\pi}}$ spectrum can be described as a reflection of the activity of the resonances in the $\mathrm{K\pi}$ system is ruled out with high significance.

Quantum numbers of the X(3872) state and orbital angular momentum in its $\rho^0 J/\psi$ decays

Phys. Rev. D 92 (2015) 011102

- Previous quantum number determinations assumed that the lowest orbital angular momentum between the X(3872) decay products dominated the matrix element.
- Significant contributions from higher orbital angular amplitudes could invalidate the 1^{++} assignment. It is necessary to perform again the analysis allowing more general angular configurations.
- Using the 3.0 fb^{-1} dataset recorded by LHCb in 2011 and 2012
- 1011 ± 38 $B^+ \to K^+ X(3872)$ with $X(3872) \to J/\psi \pi^+ \pi^-$.
- 5D analysis: all angular correlations used to measure X(3872) J^{PC}

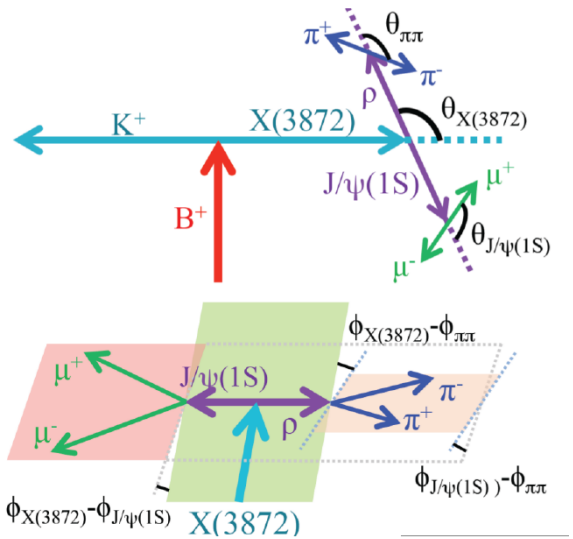

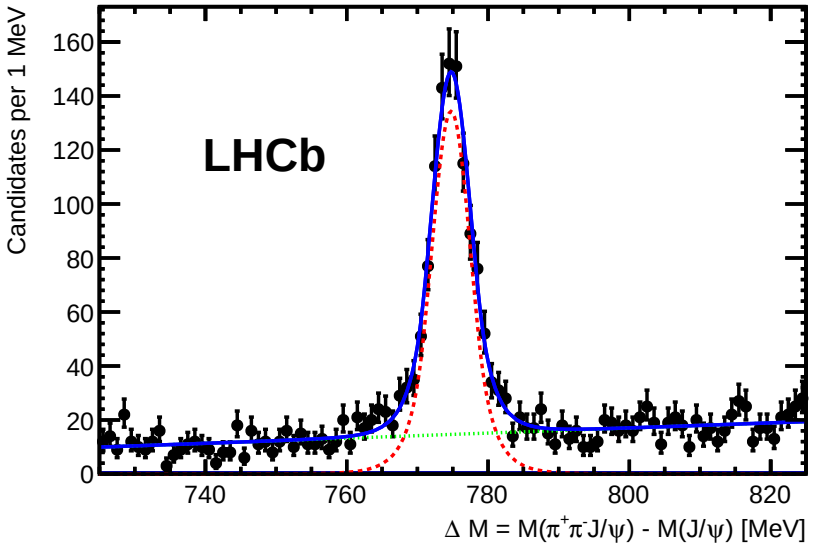

Quantum numbers of the X(3872) state and orbital angular momentum in its $\rho^0 J/\psi$ decays

Hypotesis test

- A large set of X(3872) J^{PC} configurations is considered.
- Likelihood-ratio test to discriminate between the assignments against the 1^{++};
- Results on data compared to simulated experiments.
- Data favour the 1^{++} over the alternative hypothesis with $> 16.0\sigma$;
- No significant D-wave fraction is found, with an upper limit of 0.4% at 95% C.L.

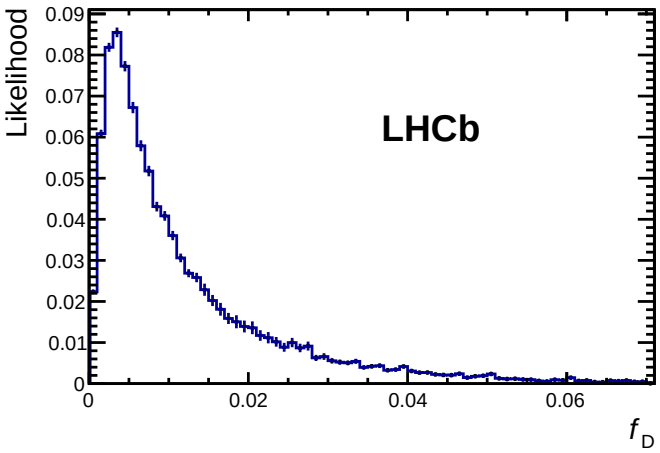

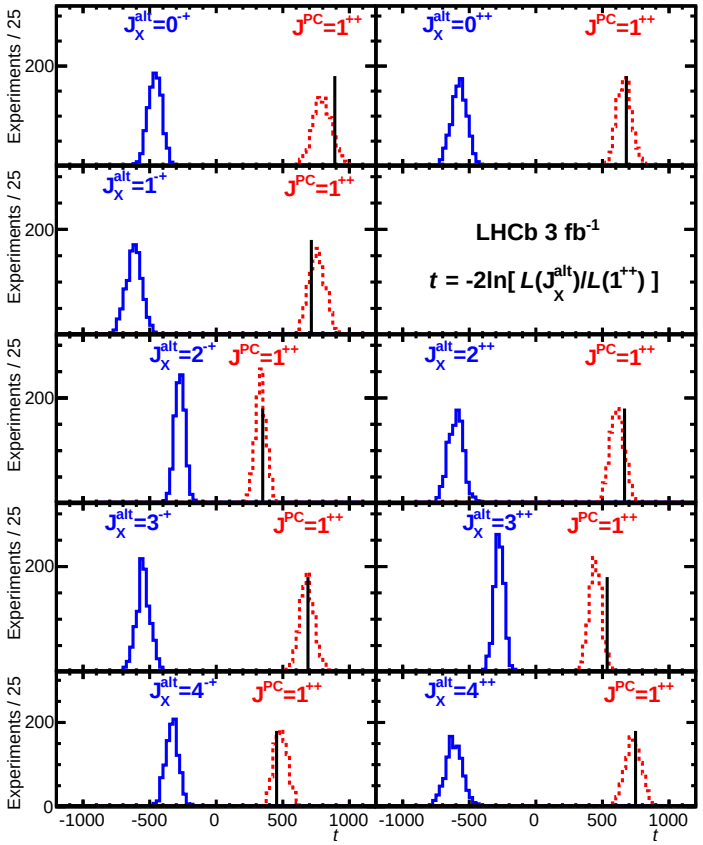

$\mathrm{X}(3872)$ production studies at LHCb

At LHCb, the $\mathrm{X}(3872)$ can be studied using:

- Prompt candidates: higher statistics but large combinatorial background.
- Candidates from B decays: lower statistics but more clear samples
- Both kinds of candidates (inclusive selection)

$\mathrm{X}(3872)$ production studies at LHCb were performed:

- Measuring the product of production cross-section multiplied by branching ratio to $\mathrm{X}(3872) \to \mathrm{J}/\psi\,\pi^+\pi^-$
- Assuming $\mathrm{X}(3872)$ as a 1^{++} state
- Performing an inclusive selection of $\mathrm{X}(3872) \to \mathrm{J}/\psi\,\pi^+\pi^-$ final state
- Fiducial range: $5 < p_{\mathrm{T}} < 20\ \mathrm{GeV}$ and $2.5 < y < 4.5$
- Efficiency estimated from Monte Carlo

X(3872) production studies at LHCb

Analysis performed on data sample with integrated luminosity of 34.7 pb^{-1} collected by the LHCb experiment in pp collisions at $\sqrt{s} = 7\ \mathrm{TeV}$ in 2010. [Eur. Phys. J. C. 72 (2012) 1972]

$$\sigma(\mathrm{pp} \to \mathrm{X}(3872) + \cdots) \times \mathcal{B}(\mathrm{X}(3872) \to \mathrm{J}/\psi\,\pi^+\pi^-) = 5.4 \pm 1.3(\mathrm{stat}) \pm 0.8(\mathrm{syst})\,\mathrm{nb}$$

$$\mathrm{M}(X(3872)) = 3871.95 \pm 0.48(\mathrm{stat}) \pm 0.12(\mathrm{syst})\,\mathrm{MeV}/c^2$$

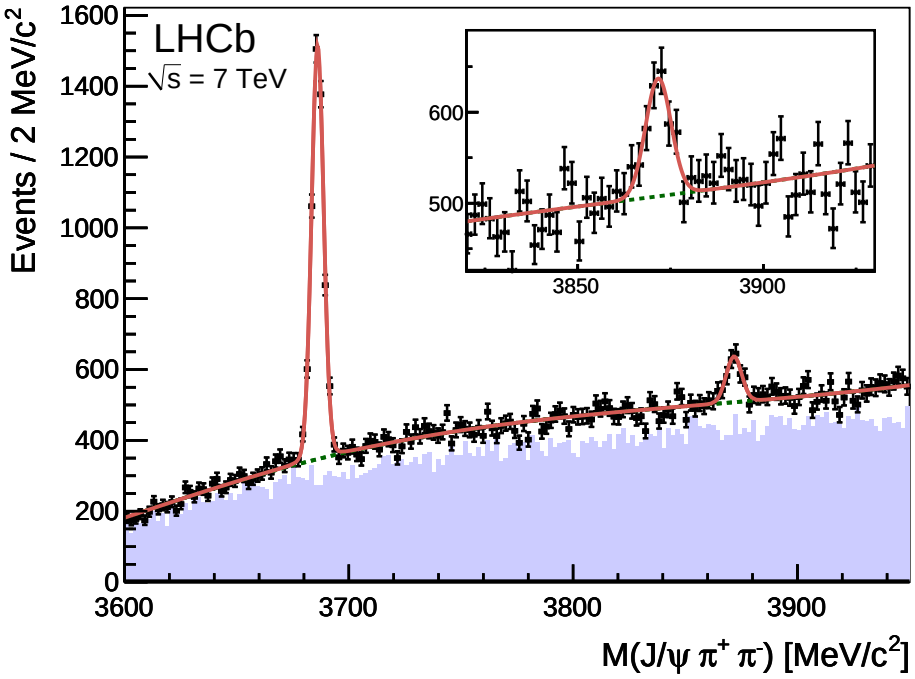

- 585 ± 74 X(3872) signal candidates
- Momentum scale calibration using $\mathrm{J}/\psi \to \mu^+\mu^-$.
- X(3872) peak fitted using a Voigt function with fixed width.
- Background studied from wrong-sign pions combinations and modeled by exponential function.
- Uncertainty dominated by statistics. It will improve with 2011 dataset

Status of X(3872) mass

- World average and $D^0\bar{D}^0*$-threshold are indistinguishable.
- Mass is a critical parameter for the $D^0\bar{D}^0*$-bound state hypotesis.
- Very low binding energy: $E_{bind} = 0.16 \pm 0.26\ \mathrm{MeV}/c^2$

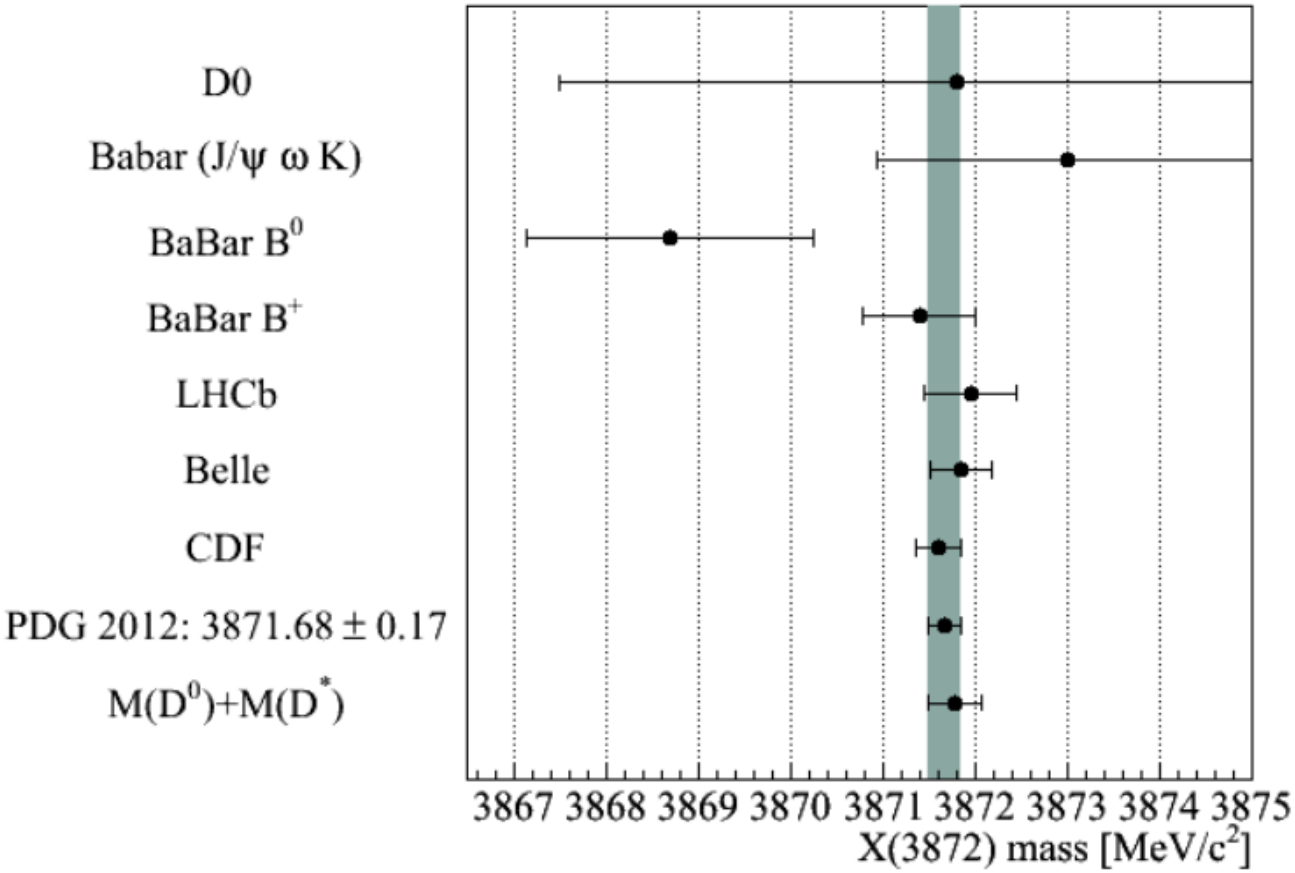

X(3872) production studies at CMS

CMS collaboration performed detailed X(3872) production studies using the decay mode $X(3872) \to J/\psi\pi^+\pi^-$, with $J/\psi \to \mu^+\mu^-$ and 4.1 fb^{-1} 7 TeV

- Measurements are performed in the range $10 < p_{T\,X(3872)} < 50$ GeV and rapidity $|y| < 1.2$.
- Detailed study of the dipion mass showing the decay proceeds dominantly through a intermediate ρ

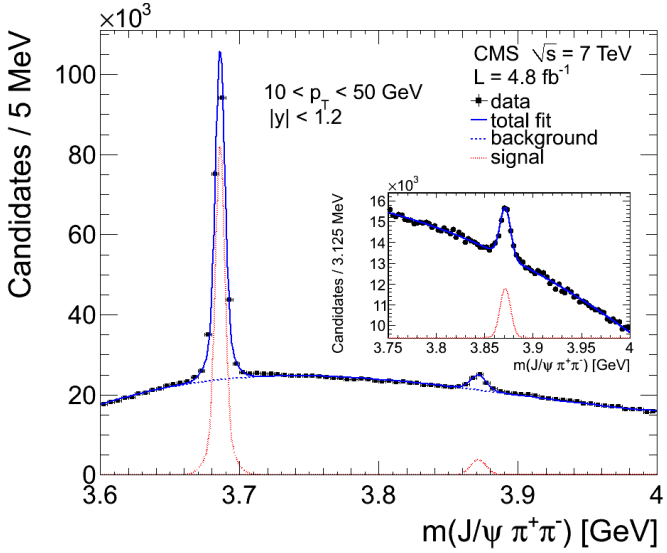

[arXiv:1302.3968]

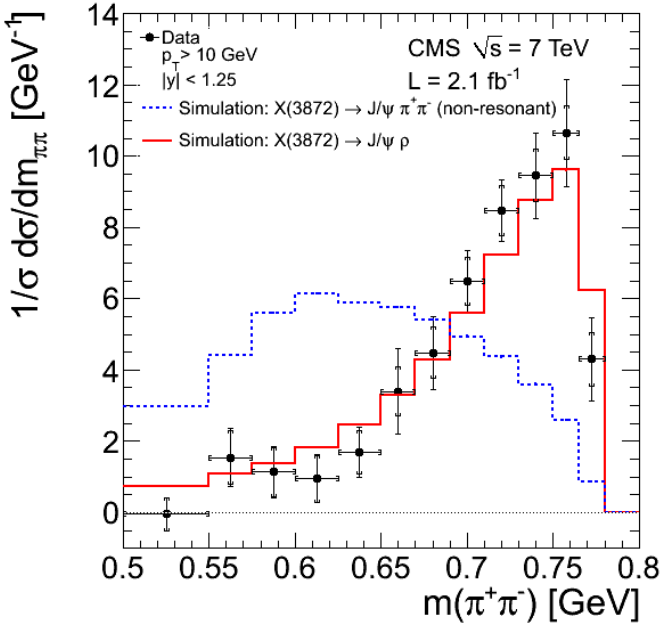

X(3872) production studies at CMS

- Ratio of the X(3872) and $\psi(2S)$ cross sections times their branching fractions into $J/\psi\,\pi^+\pi^-$ measured in function of p_T.
- Fraction of X(3872) originating from B decays.
- Prompt X(3872) differential cross section times branching fraction into $J/\psi\,\pi^+\pi^-$ and comparison with theory prediction.

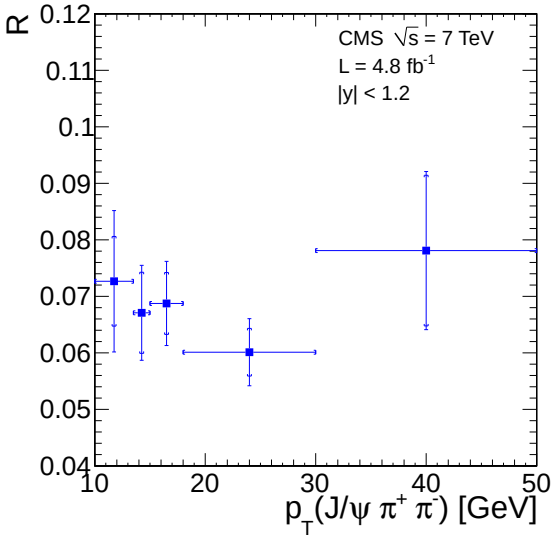

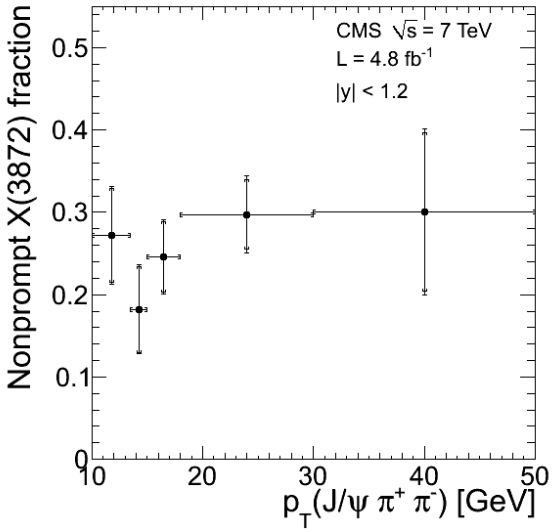

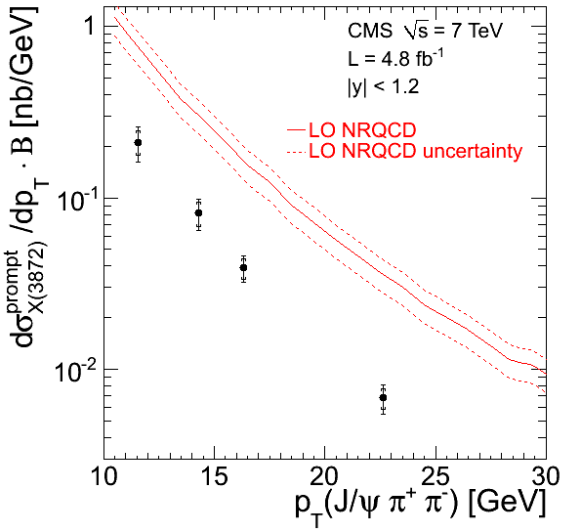

[arXiv:1302.3968]